AD-A123 722 INVESTIGATE HIGH PURITY GAAS GROWN BY MOCVD(U) ROCKWELL 1/1
INTERNATIONAL THOUSAND OAKS CA MICROELECTRONICS
RESEARCH AND DEVELOPMENT CENTER P D DAPKUS OCT 81
UNCLASSIFIED MRDC40294.2FR N00173-80-C-0066 F/G 20/2 NL

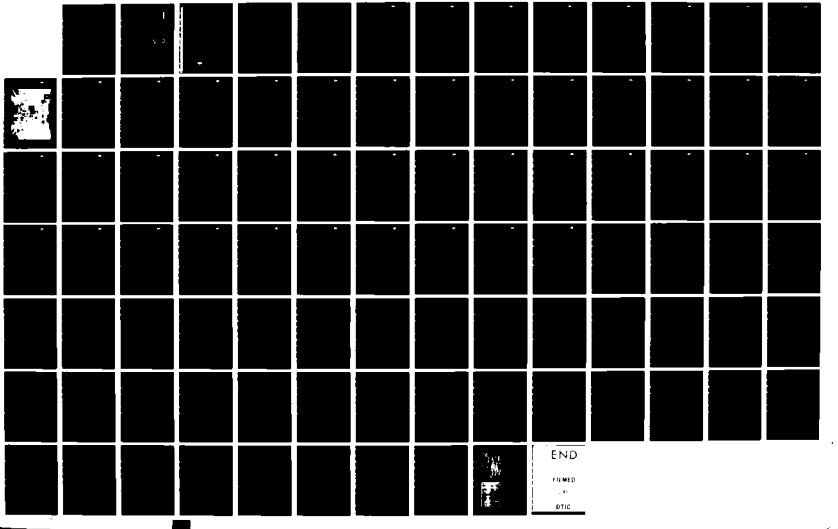

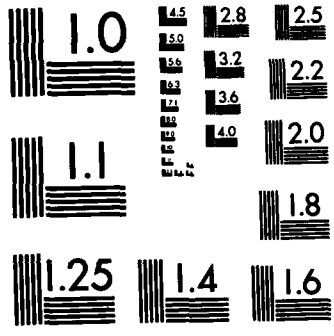

MICROCOPY RESOLUTION TEST CHART
NATIONAL BUREAU OF STANDARDS-1963-A

PHOTOGRAPH THIS SHEET

A123728

DTIC ACCESSION NUMBER

II

LEVEL

INVENTORY

Rept. No. MRDC 40294.2FR

DOCUMENT IDENTIFICATION Final, Oct. '81

Contract N00173-80-C-0066

DISTRIBUTION STATEMENT A
Approved for public release;
Distribution Unlimited

DISTRIBUTION STATEMENT

ACCESSION FOR		
NTIS	GRA&I	X
DTIC	TAB	☐
UNANNOUNCED		☐
JUSTIFICATION		
BY		
DISTRIBUTION /		
AVAILABILITY CODES		
DIST	AVAIL AND/OR SPECIAL	
A		

DTIC COPY INSPECTED 2

DISTRIBUTION STAMP

DTIC
ELECTE
S JAN 25 1983 D
D

DATE ACCESSIONED

83 01 24 503

DATE RECEIVED IN DTIC

PHOTOGRAPH THIS SHEET AND RETURN TO DTIC-DDA-2

DTIC FORM OCT 79 70A

DOCUMENT PROCESSING SHEET

MRDC40294.2FR

Copy No. 2

INVESTIGATE HIGH PURITY GaAs GROWN BY MOCVD

FINAL REPORT FOR THE PERIOD
February 6, 1980 through February 5, 1981

CONTRACT NO. N00173-80-C-0066

Prepared for

Naval Research Laboratory
Washington, D.C. 20375

P.D. Dapkus
Program Manager

OCTOBER 1981

*Approved for public release; distribution unlimited

Rockwell International

Microelectronics Research
and Development Center

UNCLASSIFIED

SECURITY CLASSIFICATION OF THIS PAGE (When Data Entered)

REPORT DOCUMENTATION PAGE		READ INSTRUCTIONS BEFORE COMPLETING FORM
1. REPORT NUMBER	2. GOVT ACCESSION NO.	3. RECIPIENT'S CATALOG NUMBER
4. TITLE (and Subtitle) High Purity GaAs Grown MOCVD		5. TYPE OF REPORT & PERIOD COVERED Final Report for Period (02/06/80-02/05/81) 6. PERFORMING ORG. REPORT NUMBER MRDC40294.2FR
7. AUTHOR(s) P.D. Dapkus		8. CONTRACT OR GRANT NUMBER(s) N00173-80-C-0066
9. PERFORMING ORGANIZATION NAME AND ADDRESS Rockwell International Science Center 1049 Camino Dos Rios Thousand Oaks, CA 91360		10. PROGRAM ELEMENT, PROJECT, TASK AREA & WORK UNIT NUMBERS
11. CONTROLLING OFFICE NAME AND ADDRESS Naval Research Laboratory Washington, D.C. 20375		12. REPORT DATE October 1981 13. NUMBER OF PAGES 88
14. MONITORING AGENCY NAME & ADDRESS(if different from Controlling Office)		15. SECURITY CLASS. (of this report) Unclassified 15a. DECLASSIFICATION/DOWNGRADING SCHEDULE

16. DISTRIBUTION STATEMENT (of this Report)

Approved for public release; distribution unlimited

17. DISTRIBUTION STATEMENT (of the abstract entered in Block 20, if different from Report)

18. SUPPLEMENTARY NOTES

19. KEY WORDS (Continue on reverse side if necessary and identify by block number)

Metalorganic chemical vapor deposition (MOCVD), GaAs, photoconductive response, emission spectroscopy, TMGa, trimethylgallium, arsine, pot residues, tail fraction, surface morphology, photoluminescence, transport properties, epitaxial materials technology.

20. ABSTRACT (Continue on reverse side if necessary and identify by block number)

An intensive study of the effects pressure on the impurity incorporation in MOCVD growth of GaAs has been undertaken. It is found that improvement in the purity of GaAs can be achieved by performing growth at reduced pressure (0.1 atm.) and that significant improvements in surface morphology also result. The total purity is however still controlled by the purity of commercially available source materials, (trimethylgallium and arsine). With the best available materials, 77°K mobilities as high as

DD FORM 1 JAN 73 1473 EDITION OF 1 NOV 65 IS OBSOLETE

UNCLASSIFIED

SECURITY CLASSIFICATION OF THIS PAGE (When Data Entered)

μ_{77} = 105,000 cm^2/V-sec were observed with reduced pressure growth compared to μ_{77} = 90,000 cm^2/V-sec for atmospheric pressure growth.

Detailed characterization of the starting materials (mass and emission spectrometry) and the resultant films (far infrared photoconductivity, photoluminescence, and transport properties) suggest that C, Si, and Zn are the dominant impurities in the GaAs grown with available materials.

Repurification of the TMGa was undertaken to understand its role in contributing to the residual background level. Different sources of TMGa were evaluated and two were chosen for repurification. Our results indicate that the best available materials are not improved much by the purification used in these studies, but substantial improvement can be made in less pure material. The highest 77K mobility observed with repurified TMGa and selected arsine was μ_{77} = 125,000 cm^2/V-sec.

TABLE OF CONTENTS

LIST OF FIGURES

LIST OF TABLES

ABSTRACT

An intensive study of the effects pressure on the impurity incorporation in MOCVD growth of GaAs has been undertaken. It is found that improvement in the purity of GaAs can be achieved by performing growth at reduced pressure (0.1 atm.) and that significant improvements in surface morphology also result. The total purity is however still controlled by the purity of commercially available source materials, (trimethylgallium and arsine). With the best available materials, 77°K mobilities as high as μ_{77} = 105,000 cm^2/V-sec were observed with reduced pressure growth compared to μ_{77} = 90,000 cm^2/V-sec for atmospheric pressure growth.

Detailed characterization of the starting materials (mass and emission spectrometry) and the resultant films (far infrared photoconductivity, photoluminescence, and transport properties) suggest that C, Si, and Zn are the dominant impurities in the GaAs grown with available materials.

Repurification of the TMGa was undertaken to understand its role in contributing to the residual background level. Different sources of TMGa were evaluated and two were chosen for repurification. Our results indicate that the best available materials are not improved much by the purification used in these studies, but substantial improvement can be made in less pure material. The highest 77K mobility observed with repurified TMGa and selected arsine was μ_{77} = 125,000 cm^2/V-sec.

1.0 INTRODUCTION

1.1 Overview

The rapid advancement of the GaAs technology during the past decade is for the first time permitting one to consider the application of signal and data processing circuits and systems operating at GHz frequencies. At present, however, there still exists a need for a high throughput controllable epitaxial materials technology for GaAs devices and circuits. This need arises from three main causes. First, the quality and reproducibility of commercially available bulk GaAs is not adequate to ensure optimal device performance reproducibly. As a result most devices are fabricated in epitaxial layers of one kind or another to isolate device performance, to the extent possible, from variations in the substrate materials. This, of course, transfers the requirements for reproducibility and control of properties to the epitaxial materials technology. The second cause relates to the need for having a well-rounded, flexible device technology in which the full potential of materials inherent properties can be utilized. That is, it will be necessary to couple a variety of technologies (epitaxy, ion implantation, fine line lithography, etc.) to achieve all the benefits of the GaAs technology. Finally, in contrast to Si, GaAs offers the possibility of forming heterojunctions with GaAlAs or other materials to provide new or improved device capabilities. Prime examples of this are the DH laser and the window solar cell both of which rely on the properties of the GaAlAs/GaAs heterojunction. The unique properties of this system have only begun to be utilized, and its use in high speed devices and circuits will become increasingly important.

Of the various epitaxial materials technologies available to day, the metalorganic chemical vapor deposition (MOCVD) process is showing promise of meeting all the needs described above. There is inherent control, scale-up potential and flexibility in the MOCVD technique. Demonstrated state-of-the-art performance in heterojunction devices of various kinds have established this technique as a potential solution to many of the needs described above.

Many problems, however, remain to be solved before the full potential of the process can be realized. Chief among these is the need to improve the purity of GaAs achievable by MOCVD. High purity materials form the basis for the controlled doping and compensation required for microwave device active layers, FET active layers, as well as buffer layers for FET devices and circuits. The goal of this study was to explore and develop techniques to grow GaAs by MOCVD of purity sufficient for the above requirements, with particular attention to microwave devices.

1.2 Contract Objective

The objective of this program was to study means for reducing the residual doping level in GaAs grown by MOCVD to levels appropriate for inclusion in microwave devices ($N_D - N_A \sim 10^{14}$ cm^{-3}). This is the final report of a 12-month program which began in February 1980.

1.3 General Technical Approach

The MOCVD process for the formation of semiconductor compounds which was developed at Rockwell over a decade ago makes use of the following simplified reaction to produce GaAs:

$$(CH_3)_3Ga + AsH_3 \xrightarrow[600\text{-}750°C]{} GaAs + 3CH_4\uparrow$$

The simplicity of this reaction provides some very important advantages for the growth of GaAs by MOCVD.

Process control is inherent in MOCVD.

1. Only a single hot-temperature zone is needed for film growth in the MOCVD process.

2. The MOCVD growth process involves reactants which are either liquid or gaseous at room temperature.

3. MOCVD provides materials and device flexibility.

MOCVD provides materials and device flexibility.

1. Doping processes and dopant sources have been identified which are considered compatible with the reactants used in the preparation of the desired GaAs films.

2. The MOCVD process is completely free of halides.

The MOCVD process is scalable to high volume.

1. Large area, uniform surface coverage in a single growth sequence can be achieved in the same type of commercial equipment that is used for the growth of elemental semiconductors.

2.0 TECHNICAL PROGRESS

This section describes the technical approach used in meeting the objective of this program. Although various task areas were addressed during the program, there was considerable overlap in these tasks. The following parts of this section, therefore, incorporate the results of studies on the tasks without identifying them separately.

2.1 Reactor Growth System

The same reactor system that was used in the earlier program was used in this program for the deposition of undoped films of GaAs from the different source batches of TMG and AsH_3. A photograph of the system is shown in Fig. 1.

The reagent handling portions of this system were fabricated from 316 stainless steel fittings, tubing and bellows-sealed valves that have been specially cleaned and tested to be leak free. Air-operated stainless steel bellows valves are used to control the reactant gas paths during a film deposition sequence. Control of these valves is accomplished via a Tylan Tymer 16 automatic valve/sequencer. The metalorganic constituents are injected into the main reactor manifold by special three-port, low-dead-volume bellows-sealed valves. This allows abrupt changes in doping and film composition to be made.

The reactor system employs electronic mass flow controllers for gas flow rate control. These mass flow controllers have a repeatability of ±0.2% full scale and regulate to within ±0.25% of the flow setting. Readout of gas flow rate is provided by a 3-1/2 digit display directly of SCCM or SLM, depending on the flow controller's range. All reactant gas flow rates are controlled by mass flow controllers. The use of these mass flow controllers and the sequencer provides the capability to grow films with excellent run-to-run doping level and thickness reproducibility.

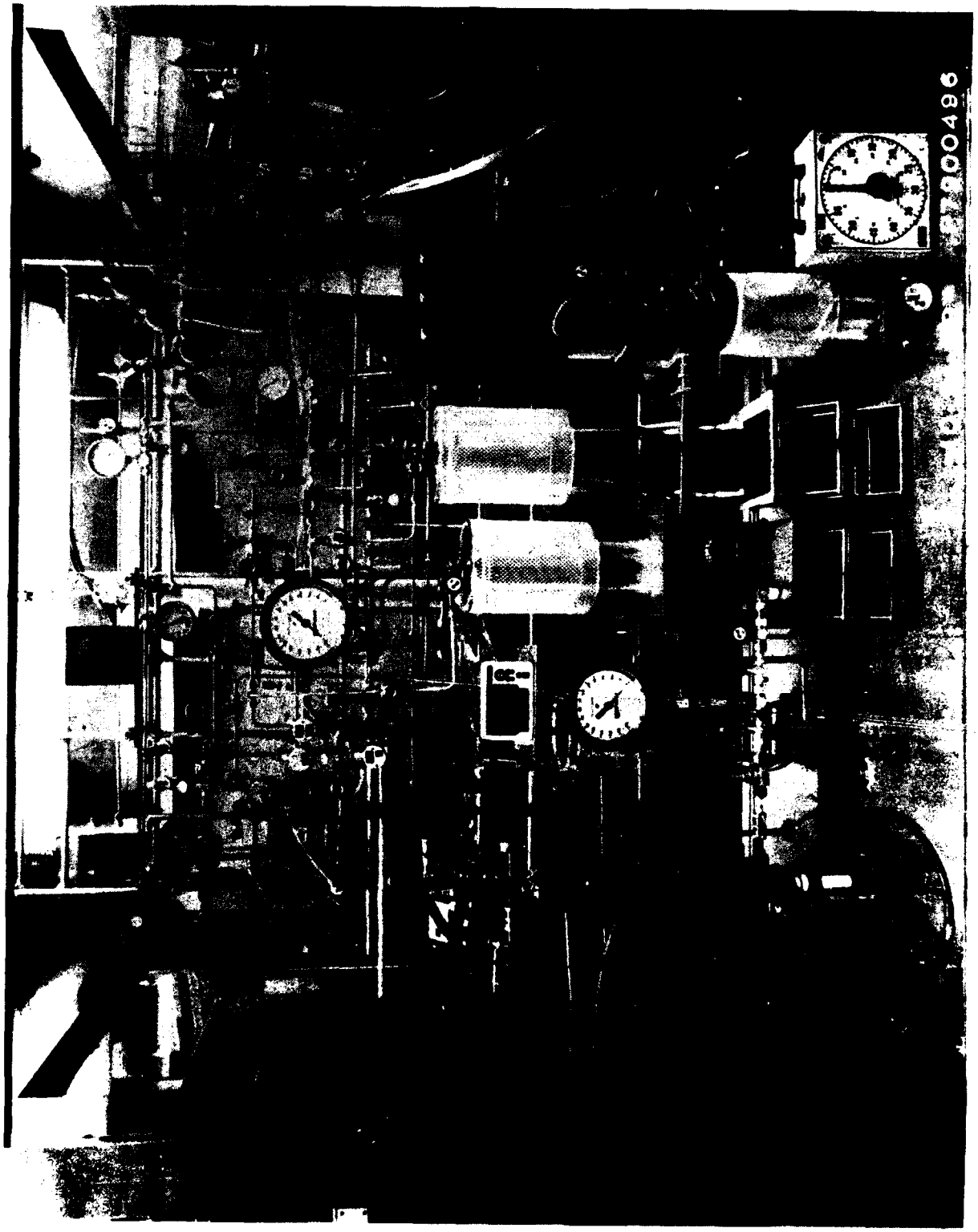

Fig. 1 Photo of reactor system apparatus.

The reactor chamber is made of high purity quartz, and the SiC-coated graphite susceptor is heated by an r-f coil external to the reactor. The temperature of the susceptor is monitored by an infrared thermometer having a digital readout. The quartz chamber is specially designed to produce extremely uniform and homogeneous films over a 20 cm^2 area.

This reactor system also includes a vacuum system employing a direct drive chemical-resistant vacuum pump. This vacuum capability is used to evacuate the quartz reactor chamber prior to each growth run and to aid in leak checking the reactor gas lines.

This vacuum pump is used in combination with liquid N_2 baths for the reduced pressure studies. The pressure in the growth apparatus is monitored by appropriate pressure-vacuum type guages.

Provisions for collecting and/or sampling condensates from the source materials for subsequent analysis and/or use are also built into the system.

A 48 liter-per-minute capacity palladium element H_2 purifier provides UHP H_2 for the reactor system. The UHP H_2 supply line and all other gaseous source lines have low temperature traps (the H_2 trap employs LN_2; the others are controlled by thermostatic coolers) to remove traces of moisture from the gas supplies.

The reagent handling portion of this reactor system is enclosed in a specially fabricated safety cabinet having its own independent exhaust blower and exhaust failure warning system.

2.2 Comparison of Atmospheric and Reduced Pressure MOCVD Growth

In this section, we will describe the specific procedures used for the growth of GaAs at reduced and atmospheric pressure. A detailed comparison of the materials characteristics is given in the Appendix I publication.

2.2.1 Substrate Preparation and Reactor Cleaning

The substrates used in this study were obtained both from commercial vendors and Rockwells in-house facility. The substrates were purchased with a thickness of 0.030" and were bulk etched in 3:1:1 H_2SO_4:H_2O_2:H_2O to remove 0.010". They were then lapped to 0.012"-0.015" thickness by removing an equal amount from each side. One side was then polished. Final wafer thickness was 0.010"-0.012. The wafers were cleaned prior to insertion into the reactor using the following procedure:

1. 5 min. Boiling trichloroethane
2. 5 min. Boiling dimethylketone
3. 5 min. Boiling 2-propanol
4. Deionized water rinse
5. 2 min. 1:1:10 H_2O:H_2O_2:H_2SO_4
6. Deionized water rinse
7. 5 min. Hot HCl (aq)
8. Deionized water rinsed
9. N_2 blow dry

All reactor parts are cleaned with an etch in 2:9 HF:HNO_3. The quartz parts are rinsed in deionized water and blown dry. The susceptor is rinsed in methanol and blown dry. The substrate is positioned on the susceptor and the reactor assembled and evacuated to 0.001 atm through a 77°K cold trap for 30 min. All of the above procedures are followed regardless of the mode of growth.

2.2.2 Growth Procedures

For atmospheric pressure growth, the temperature of the susceptor is increased to 550-600°C under hydrogen at which time 500 cc of 10% arsine is admitted into the reactor to stabilize the GaAs. After 2 min TMGa is admitted into the reactor to begin growth.

For reduced pressure growth, 1 Lpm of H_2 is metered into the reactor at the metering valve at the inlet of the reactor. The working pressure is then established by introducing ultrapure N_2 into the exhaust line of the reactor. The reactant gas manifold pressure is maintained at >1 atm, the reactor at the required working pressure and the flow rates at the specified values. Once established, these conditions are quite stable.

After growth, the crystals are cooled to room temperature in 550 ccpm 10% arsine and purged with H_2 before removal from the reactor.

2.2.3 Results Obtained with Reduced Pressure Growth

The major effect observed with reduced pressure growth was the reduction of the total impurity content of the GaAs films. The effect did not appear to be selective to one impurity over another. The effect is believed to be the result of decreased residence time of the spent reactants over the substrate. The detailed characteristics of reduced pressure growth and a comparison of it with atmospheric pressure growth is given in Appendix I and will not be repeated here.

2.3 Repurification Apparatus and Techniques

The purification of commercially available TMGa was performed in a specially designed quartz apparatus. A schematic diagram of the apparatus is illustrated in Fig. 2. The major components of this apparatus include a high efficiency packed fractional distillation column which is directly interfaced with a multi-purpose chemical vacuum line.

The vacuum system was used for the quantitative measurement and handling of both condensable and noncondensable gases, separation of volatile compounds by standard low temperature/low pressure techniques, storage and transfer of volatile liquids and gases, and a wide range of analytical work. The system used high vacuum greaseless stop-cocks, and had provision for delivering argon gas with purities in excess of 99.9999% (R. D. Mathis Argon Gas Purifier). The UHP argon was used for overpressurizing cylinders and

SC81-14759

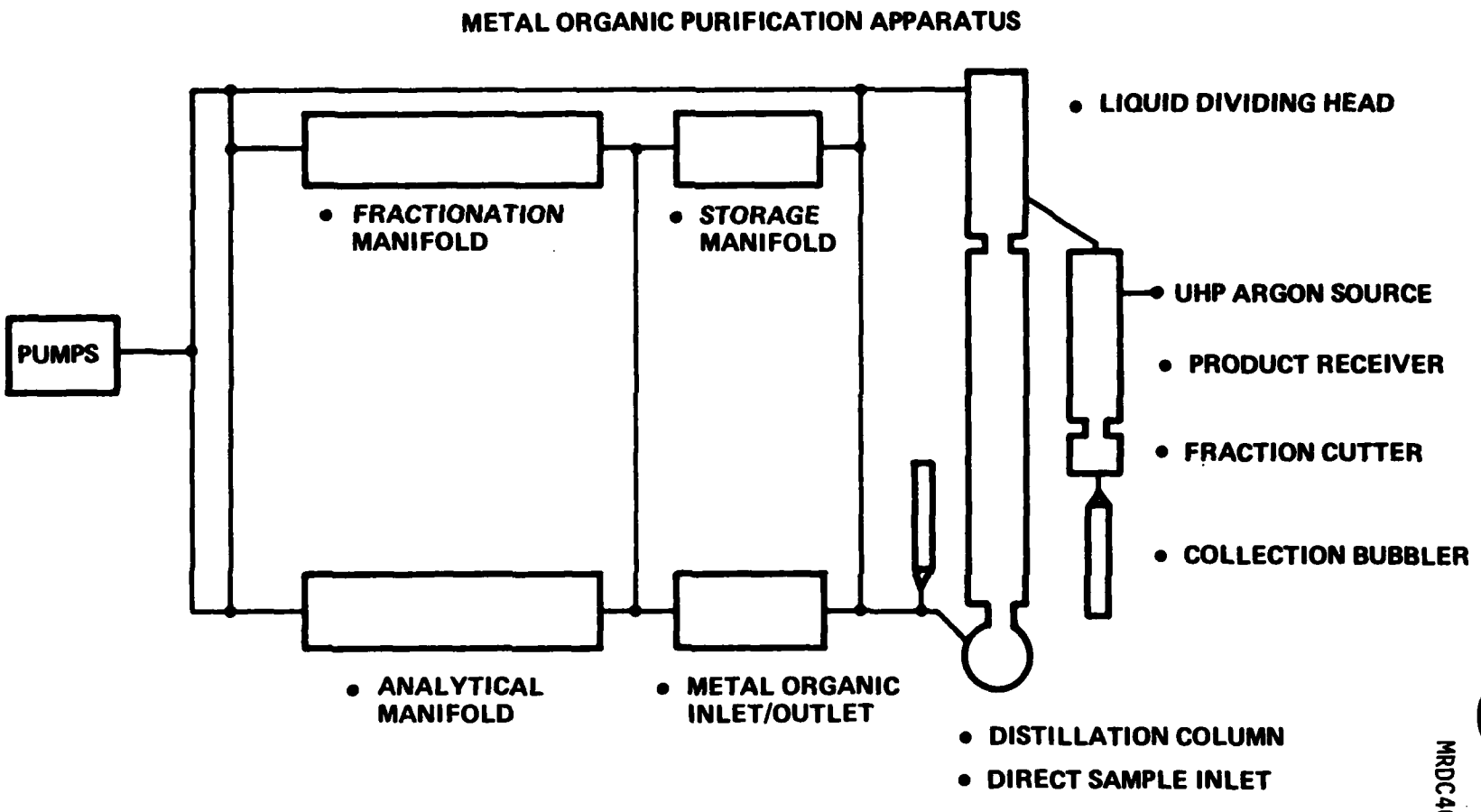

Fig. 2 Metal organic purification apparatus.

sample tubes and for providing an inert gas blanket under which the atmospheric pressure distillations could be performed.

The quartz distillation apparatus was composed of the following functional units: (1) distillation pot, (2) packed fractionation column, (3) automatic liquid dividing head, (4) product receiver and fraction cutter, and (5) metal alkyl collection receivers. The distillation pot was designed to maintain a satisfactory evaporating area during the distillation in comparison to the cross-sectional area of the fractionation column. An externally controlled heating element was used to provide an evenly heated surface which prevented local overheating of the TMGa source materials. A unitized thermowell/thermocouple combination was used to monitor the temperature of the TMGa in the pot during the distillation and was helpful in reducing the ΔT between the pot and automatic liquid dividing head where the repurified material was concentrated. A specially designed quartz/stainless steel inlet sidearm permitted gravity transfer of the reactive TMGa into the distillation pot directly from the vacuum line.

The fractionation of the TMGa source materials was carried out inside a three foot long vacuum jacketed and silvered column which operated adiabatically throughout its length. The internal column dimensions (12 mm I.D.) allowed efficient contacting of the rising TMGa vapors and returning reflux which maximized the exchange between heat and material. A low pressure drop along the length of the column made it desirable for low pressure distillation of metal alkyls when necessary. The column was packed with ~5100 quartz helices.

These helices (4 mm O.D. × 3 mm I.D. × 1/16" thick) exhibited a large surface area/volume ratio. They were capable of equilibrating a large volume of vapor/liquid per unit time because of the small liquid hold-up per individual helice and the efficient throughput provided by the free space of the helice network.

The automatic liquid dividing heat which acted as the "second stage" in the distillation apparatus was also vacuum jacketed and silvered to mini-

mize heat loss during product equilibration and recovery. A unitized thermowell/thermocouple assembly, which was continually bathed in the vapors of the product material, provided an uninterrupted digital display of distillate temperature. A coiled total condenser (water cooled) was used to minimize partial reblending of components. The entire assembly was coupled to a timer controlled magnetic solenoid which activated the distillate recovery mechanism, and helped maintain precise control of the reflux ratio during the repurification. The head was directly interfaced to the UHP argon source via a pressure equilization manifold.

The product receiver and fraction cutter were water cooled to minimize volatilization of product cuts during collection. The pressure equalized fraction cutter directed the flow of repurified TMGa into either 316 SS electron beam welded source bubblers or high purity quartz bubblers.

Atmospheric pressure distillation (argon blanket) was used exclusively in this limited study because of the high volatility of the TMGa source materials and high degree of impurity separation which could be achieved by this process.

Prior to each distillation, the apparatus was evacuated ($\sim 10^{-6}$ torr) for 24 hours). The quartz surface was then passivated at room temperature with the vapor of TMGa (stored in a bulb on the vacuum line at 0°C; vapor pressure of TMGa ≈64 torr). The passivation converted reactive ≡ Si-OH and ≡ Si-O-Si ≡ linkages into ≡ Si-O-Ga$(CH_3)_2$ and ≡ Si-CH_3 networks, i.e.,

$$\equiv \text{Si-OH} + (CH_3)_3Ga \longrightarrow \equiv \text{Si-O-Ga}(CH_3)_2 + CH_4 \qquad (1)$$

$$\equiv \text{Si-O-Si} \equiv + (CH_3)_3Ga \longrightarrow \equiv \text{Si-O-Ga}(CH_3)_2 + \equiv \text{Si-}CH_3 \qquad (2)$$

Surface passivation was considered complete when no further methane (CH_4) could be pumped from the apparatus, although more time was usually allowed for the slower reaction (2) to equilibrate and come to completion.

TMGa was then gravity transferred from the vacuum line into the distillation pot through the quartz/stainless steel interface valve. A small aliquot of this TMGa was also collected in a 316 SS sample cylinder for subsequent analysis by mass spectroscopy. A blanket gas of UHP argon was used throughout the entire fill procedure and distillation process. A safety bubbler containing pentaphenyl trimethyl trisiloxane (extrapolated vapor pressure at 25°C ≈ 5×10^{-7} torr) isolated the constituents of the distillation environment from the atmosphere.

Three fractions were collected during each distillation, and these were subsequently evaluated using optimized MOCVD "use test" growth parameters. Selected fractions were also analyzed by mass spectroscopy.

The column hold-up material and any high boiling contaminants which were concentrated in the still pot were pumped into a -198°C storage bulb on the vacuum line and later fractionated using low temperature/low pressure techniques. It was found that excellent separations could be achieved if at a particular temperature the ratio of vapor pressures of two components was $>10^4$; a ratio of 10^3 usually resulted in a good separation; a ratio of 10^2 only permitted a fair separation in such cases, repeated and careful fractionation was required in order to obtain a partial separation fo impurities.

Samples of impurities isolated by this technique were collected in either stainless steel or quartz sample cylinders and subsequently analyzed by mass spectroscopy and/or emission spectroscopy depending on the volatility of the material. A summary of the repurification and characterization procedure is illustrated in Figs. 3 and 4.

2.4 Characterization Studies

2.4.1 Electrical Characterization of MOCVD Grown GaAs

The ultimate test for purity of the repurified TMGa was the MOCVD use test, i.e., the growth of thin films of GaAs and measurement of electrical transport properties at 300°K and 77°K. Experience with TMGa has determined

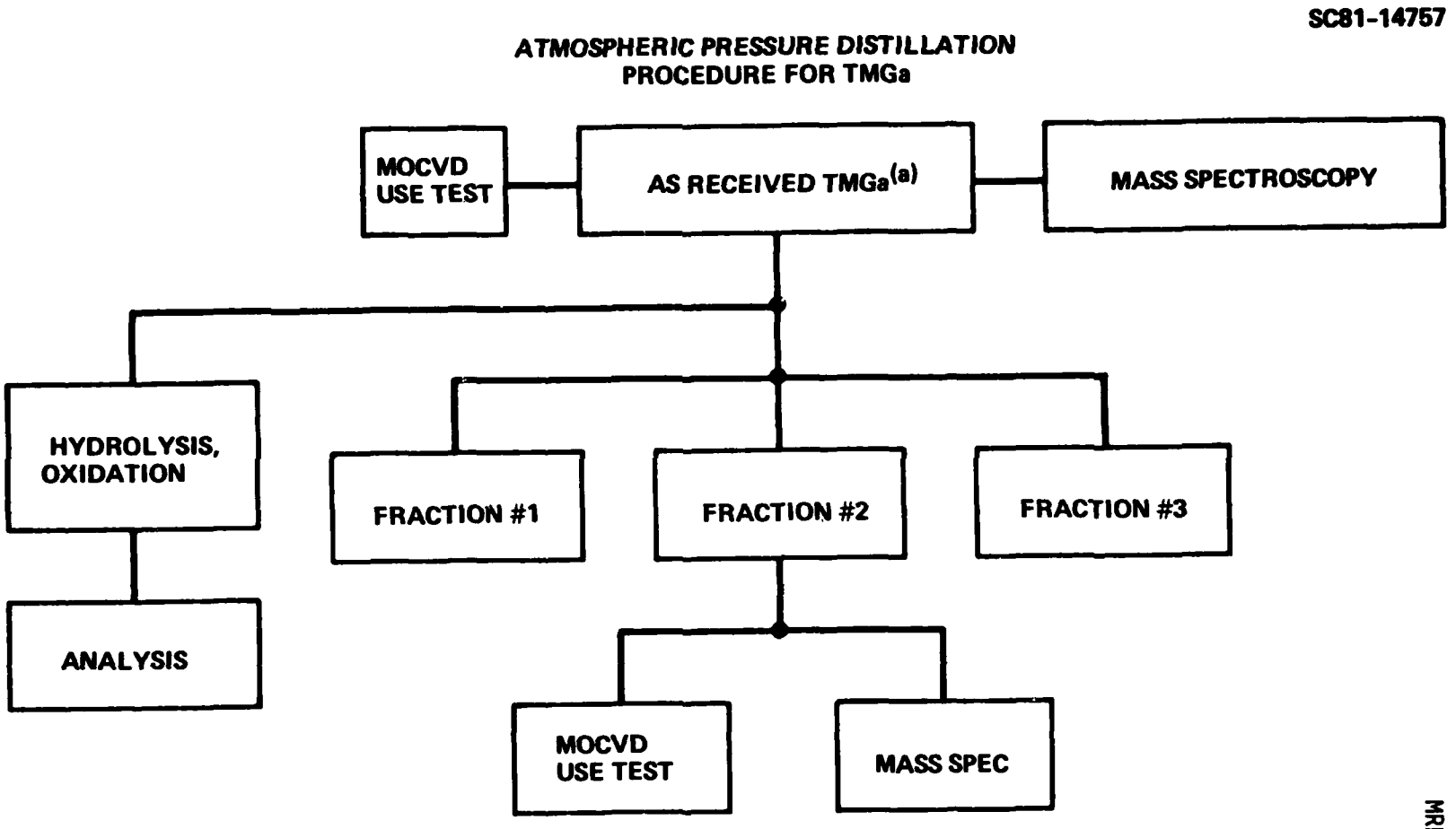

Fig. 3 Atmospheric pressure distillation procedure for TMGa.

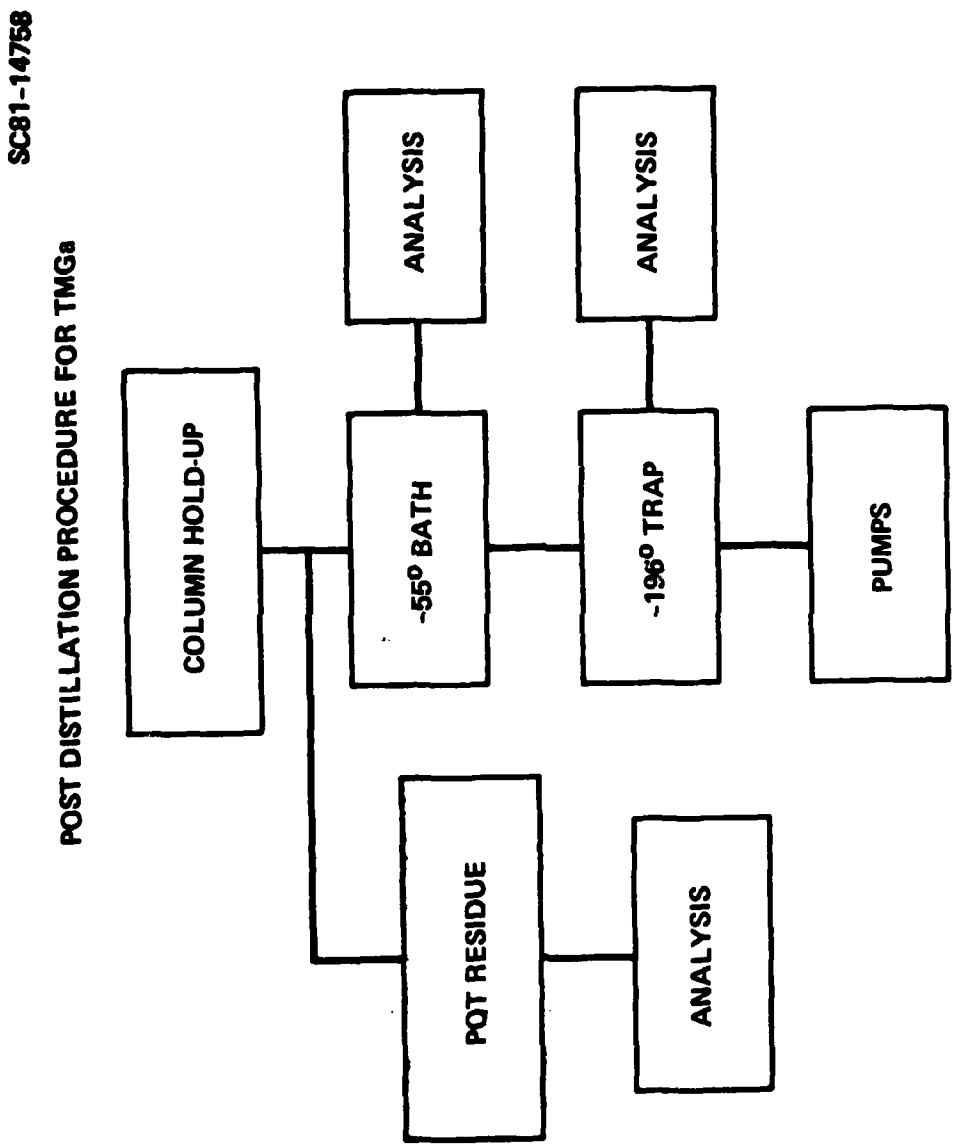

Fig. 4 Post distillation procedure for TMGa.

appropriate optimized conditions for the growth of very high quality GaAs films. These conditions are summarized in Table I. We could make definite comparisons between the properties of films produced from TMGa prior to purification and from selected fractions after distillation. This work was performed in a high purity GaAs crystal growth reactor because of its characteristic high level base line operating features.

Table I. High Purity GaAs Grown by MOCVD With Repurified Trimethylgallium

Optimized MOCVD Growth Parameters

Optimized Parameter	APMOCVD	LPMOCVD
Reactor Pressure	760 torr	70 torr
Total Gas Flow	4 lpm	1 lpm
AsH_3/H_2 Flow	500 ccpm	500 ccpm
$H_2/(CH_3)_3Ga$ Flow	15 ccpm	10 ccpm
$(CH)_3Ga$ Source (°C)	0°C	-12°C
Growth Temperature	600°C	575-600°C
Growth Rate	0.166 μm/min	0.055 μm/min

The GaAs samples grown in this study were then characterized using van der Pauw geometry Hall effect measurements. These measurements were performed on rectangular samples by contacting them with indium dots around the periphery of the sample. Care was taken to avoid edge leakage effects in high resistivity samples. The Hall effect was measured in an automated Hall apparatus utilizing a 5 kg magnetic field. 77°K measurements were performed immersing the sample in liquid nitrogen. Temperature dependent measurements were made in the same automated apparatus by heating the sample immersed in the vapors from liquid nitrogen. Temperature dependent measurements had an accuracy of ±1°C.

2.4.2 Donor Spectroscopy

The residual donor species present in the undoped GaAs were identified by far infrared photoconductivity measurements. This technique is based on the photothermal ionization of neutral donor species in GaAs. Donors in GaAs are known to be hydrogenic impurities. The ground state of each specific donor, however, is slightly modified by central core effects specific to each particular impurity. Therefore, the energy between the ground state and the first excited state of each donor impurity is found to vary from donor to donor. These energies have been carefully catalogued by several workers with the net result that a positive identification of the donor in GaAs can be achieved provided that the concentration of donors and acceptors is low enough to avoid smearing of the transitions due to localized electric field effects and screening.

Implementation of far infrared photoconductivity for donor spectroscopy is carried out by immersing a sample cooled to liquid helium temperatures in a magnetic field such that the transition between the ground state and various excited states are split owing to the Zeeman effect. A tunable far infrared light source is then directed on the sample, and the change in the conductivity as a function of the wavelength of the tunable source is measured at 4°K. There is sufficient thermal energy available to excite an electron from an excited state of the donor into the conduction band, but less than that required to excite an electron from the ground state to the conduction band. By concentrating on one of these transitions, namely, the $1S_0 \rightarrow 2P_{-1}$ transition, the extrinsic photoconductivity shows a series of peaks owing to transitions from the ground state to the various spin levels of the excited state.

High resolution photoconductivity measurements can identify transitions occurring on different donor species within the material. If the doping is sufficiently low, these transitions are sharp, and the donor species can be clearly identified. The data to be presented in this contract report were accumulated utilizing a magnetic field of 65 kg. The resulting wave number

for the $1S_0 \rightarrow 2P_{-1}$ transition is shown in Table II. These energies are based on previous work by Stillman and co-workers.[4-6] Though some of these energies may be viewed as tentative, the majority are well accepted, and in cases where controversy exists, the data presented in this contract report will help clarify their identification. Figures 5 and 6 show a schematic diagram of the photothermal ionization process utilized in the far infrared photoconductivity measurements as well as the photoconductivity spectra of a sample with and without an applied magnetic field. It is the $1S_0 \rightarrow 2P_{-1}$ transition that is studied in detail in this report to determine the specific donor species.

Table II. Energy of 1S-2P (m = 1) Transition (65 kg) for Various Donors in GaAs

Pb	35.0 cm^{-1}
X_1(1)	35.3 cm^{-1}
Se	35.42 cm^{-1}
Sn	35.50 cm^{-1}
Si	35.90 cm^{-1}
S	36.37 cm^{-1}
C(2)	36.82 cm^{-1}
Ge(2)	36.7 cm^{-1}

(1) X_1 is a donor level observed in a variety of GaAs materials and is believed to be associated with Ga in vacancy complex.

(2) There is some ambiguity in the identification of C and Ge donors. Recent work[i] identified the X_3 peak of Stillman, et al.[ii] as due to Ge. The present work corroborates Stillman's early identification of X_3 as being C.

i. M. Ozeki, et al., Jpn J. Appl. Phys., 16, 1617 (1977).

ii. C. M. Wolfe, et al., Proceedings of the GaAs and Related Compounds Conference, St. Louis, 1976, Inst. of Phys., London and Bristol, p. 120.

SC81-14756

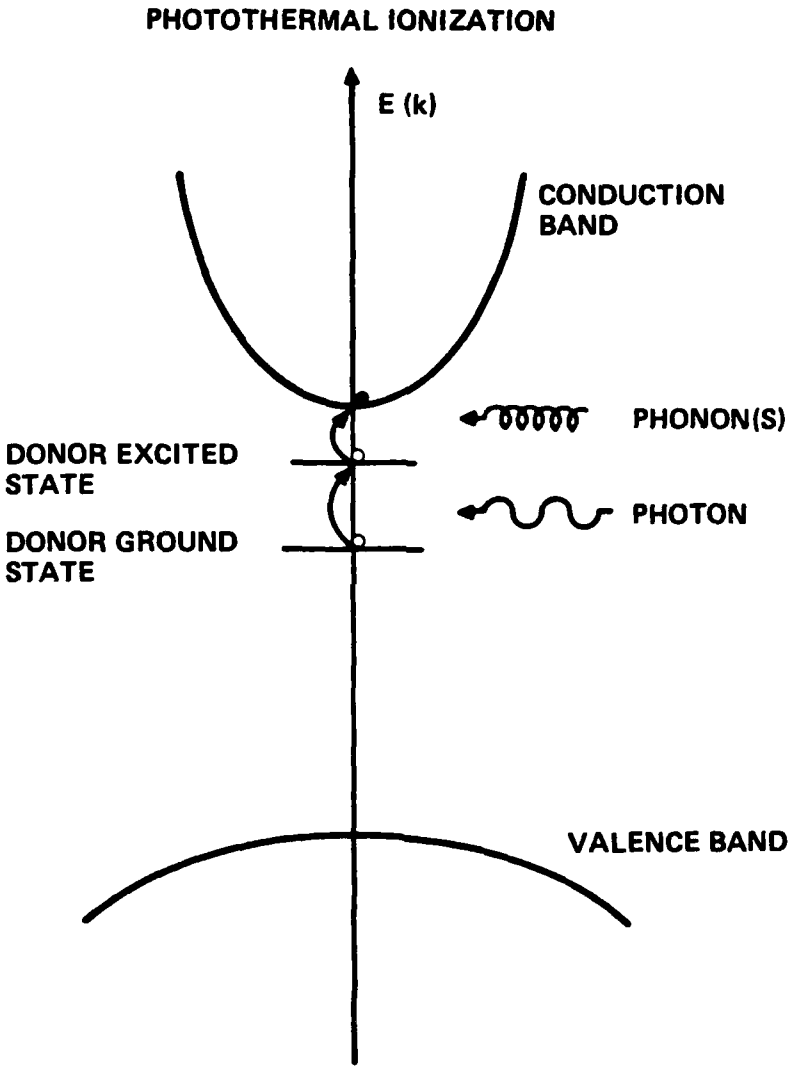

Fig. 5 Photothermal ionization.

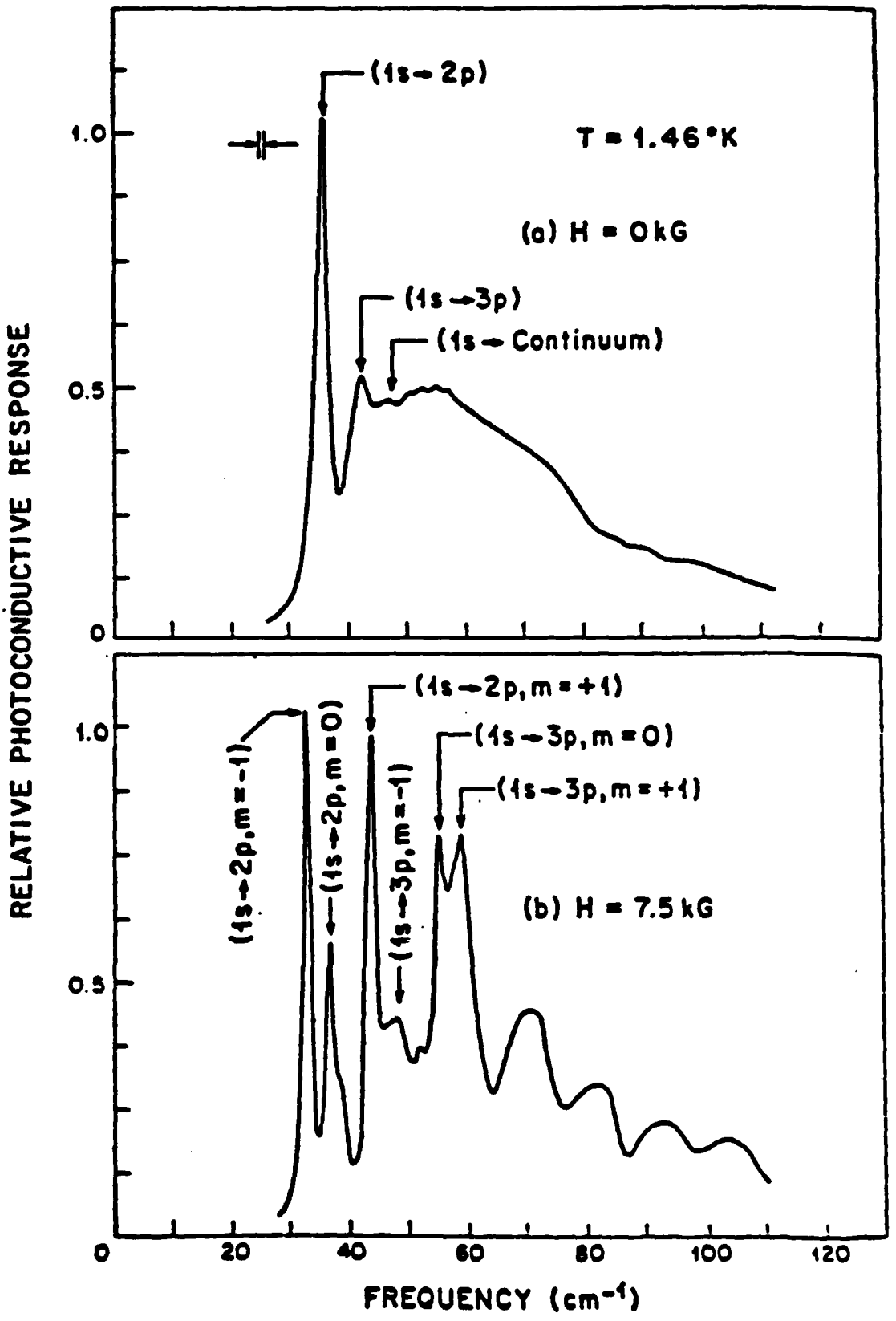

Fig. 6 Relative photoconductive response.

2.4.3 Mass Spectroscopy (Qualitative)

The mass spectra of the TMGa source materials and isolated contaminants were recorded on a low resolution Hitachi-Perkin Elmer RMU-6D magnetic sector mass spectrometer by West Coast Technical Services in Cerritos, California. Trimethylgallium was identified from its molecular ion and three fragment ions. These data are summarized in Table III. All four patterns had the correct isotopic ratio characteristic of the two stable isotopes for gallium.

Table III. Identification of Trimethylgallium

Specie	m/e	Abundance
*$Ga^{71}(CH_3)_3$	116	4th
$Ga^{69}(CH_3)_3$	111	"
$Ga^{71}(CH_3)_2^+$)	101	1st
$Ga^{69}(CH_3)_2^+$	99	"
$Ga^{71}(CH_3)^+$	86	3rd
$Ga^{69}(CH_3)^+$	84	"
Ga^{71+}	71	2nd
Ga^{69+}	69	"

*Ga^{71} 40% natural abundance
Ga^{69} 60% natural abundance

Normal saturated hydrocarbons C_NH_{2N+2} ($N > 5$) were identified from the characteristic clusters of peaks, 14 mass units (CH_2) apart, of decreasing intensity with increasing fragment length. In each case the molecular ion peak was always present albeit of low intensity. For unsaturated hydrocarbons C_NH_{2N} ($N < 5$) the molecular ion peak, apparently formed by removal of a π-electron, was usually distinct. The prominent peaks from these mono-olefins

exhibited the general formula C_NH_{2N-1} (alkyl carbonium ions), but fragments of the composition C_NH_{2N} formed in McLafferty rearrangements were also found.

For aliphatic ether linkage R-$\ddot{O}$-R' the parent peak at m/e-46 (two mass units larger than the corresponding hydrocarbon) was small in comparison to the major (P-1) peak at m/e-45. The presence of an oxygen atom was deduced from strong peaks at m/e-31 and m/e-45. These intense peaks represented the $CH_3O^{\cdot +}$ and $CH_3OCH_2^{\cdot +}$ fragments. A lack of major peaks at m/e-59, m/e-73, etc. clearly established the R-$\ddot{O}$-R' linkages as CH_3OCH_3, compared to longer chain ethers.

Alkyl halides, in particular methyl iodide, was easily identified primarily through the presence of the strong molecular ion parent peak at m/e-142 and the corresponding fragment ion at m/e-127 due to mono-iostopic iodine.

2.4.4 Emission Spectroscopy

Metal and nonmetal microimpurities were identified by emission spectroscopy at Spectrochemical Laboratories in Los Angeles, California. Figure 7 summarizes the elements detectable and limits of detectability using this technique.

2.5 Experimental Results

2.5.1 Evaluation of As-Received TMGa Source Materials

Two sources of TMGa from different commercial vendors (TMGa-A, foreign source; TMGa-B, domestic source) were evaluated by the MOCVD use test and mass spectroscopy prior to repurification. The electrical transport properties of undoped GaAs films grown with these two sources using optimized deposition parameters are summarized in Table IV. The GaAs grown with the TMGa-A source is low purity with $\mu_{77°K} \approx 30{,}000$ being independent of the growth technique used. The relatively high n-type doping density ($\sim 3 \times 10^{15}$ cm^{-3}) for these films corresponds to a high total ionized impurity concentration ($\sim 7 \times 10^{15}$ cm$^{-3} \approx N_D + N_A$).

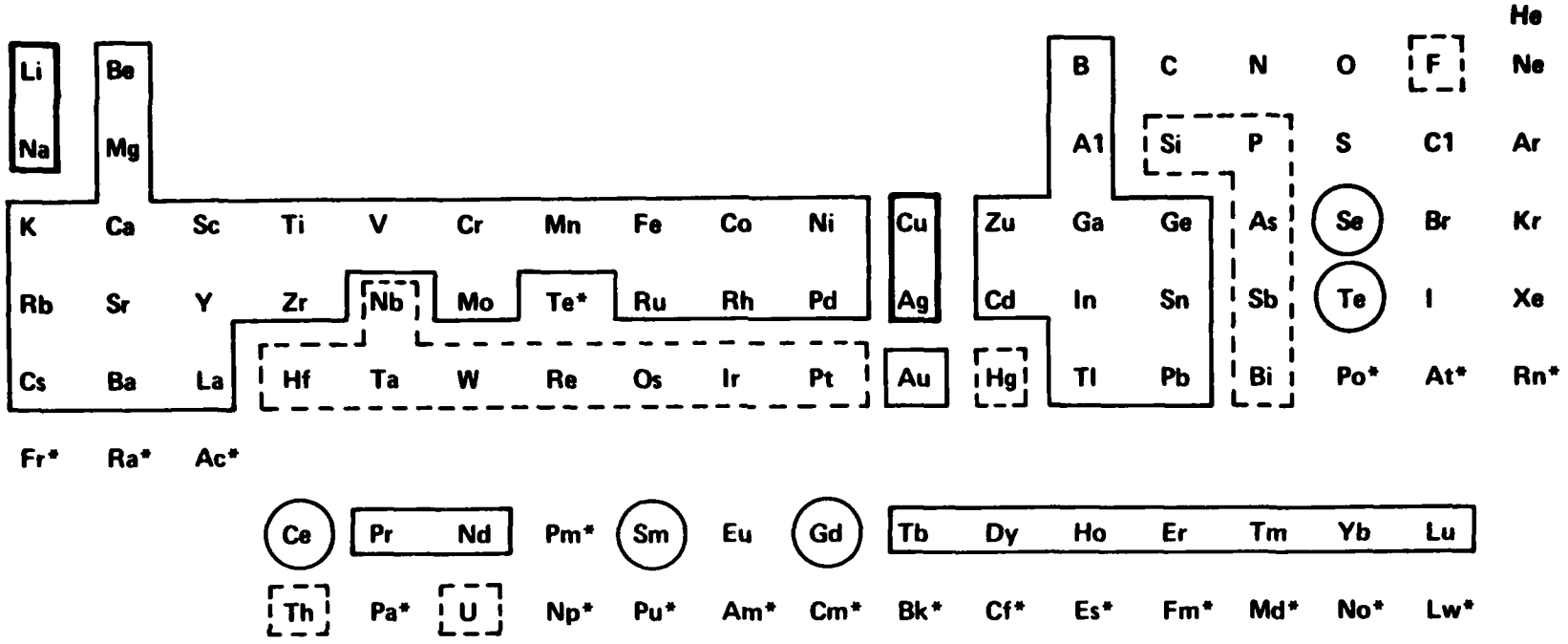

LIMITS OF DETECTABILITY

- ——— < 1 ppm
- ——— 1-10 ppm
- - - - - 10-100 ppm
- ○ 100-1000 ppm
- * RADIOISOTOPES

Fig. 7 Elements and detectability limits for emission spectroscopy.

Table IV. Electrical Properties of GaAs Grown by MOCVD With As-Received Trimethylgallium Source Materials

Property	Source-A		Source-B	
Mobility at 77°K[a]	28,840	31,522	87,471	89,438[b]
$(N_D - N_A)$ at 77°K	2.9×10^{15}	3.4×10^{15}	2.4×10^{14}	3.9×10^{14}
$(N_D + N_A)$ at 77°K	7.4×10^{15}	6.5×10^{15}	1.1×10^{15}	9.0×10^{14}
$AsH_3/(CH_3)_3Ga$	~40/1	~103/1	~40/1	~103/1
Technique	APMOCVD	LPMOCVD	APMOCVD	LPMOCVD

[a] Film thickness for all sample ~20 μm.

[b] $\mu(77°K) \approx 107{,}532$ $cm^2/V\text{-sec}$ at growth temperature ~575°C.

In comparison the GaAs films grown with the TMGa-B source were high quality with $\mu_{77°K} \approx 90{,}000$ again being independent of the growth technique. The low n-type doping density ($\sim 3 \times 10^{14}$ cm^{-3}) is approximately an order of magnitude lower than that obtained from the TMGa-A source and corresponds to total ionized impurity levels $N_D + N_A \approx 10^{15} \times 1$. These results for films grown at atmospheric and low pressure attest to the good quality of the domestic source material in comparison with the foreign TMGa.

The TMGa-A material was selected as the prime candidate for repurification, with the purification results expected to indicate a more dramatic improvement in GaAs film properties than would be obtained with the domestic source. Both of these TMGa samples were first analyzed for major contaminants by low resolution mass spectroscopy, and the results of these analyses presented in Table V.

Both source materials exhibited all four cracking patterns characteristic of TMGa with the correct isotopic ratio distribution for the two stable gallium isotopes (Ga^{71}, 40%; Ga^{69}, 60%). These results indicate the absence of any associated gallium species, i.e., parent trimer ions

Table V. Qualitative Mass Spectrometric Analysis of As-Received Trimethylgallium Source Materials

TMGa-A Gas Phase Composition	TMGa-B Gas Phase Composition
$(CH_3)_3Ga$	$(CH_3)_3Ga$
CH_3I	CH_3OH*
CH_4	CH_4
C_5H_{10}	H_2
C_NH_{2N+2}, C_NH_{2N} } $N \leq 5$	
H_2	

*Could not exist as contaminant in TMGa source material due to reaction CH_3OH + Excess $(CH_3)_3Ga$ → $(CH_3)_2GaOH$ + CH_4...

$[(CH_3)_3Ga]_3^+$. There were no molecular or fragment ions characteristic of any Group 3 metal alkyl contaminants despite the progressive decrease in M-C bond strengths between boron and thallium. Such molecular ion abundances would have been expected to follow the order Al>B>Ga>In>Th had they been present to a significant extent in the gallium source materials.

Methyliodide was identified to be the major contaminant in the TMGa source material. Although the synthetic history of the MOCVD-A batch is unknown, it is possible to rationalize the presence of the CH_3I by considering three commonly used syntheses of TMG. These routes are summarized in Table VI. All three methods involve CH_3I in quantities which are greater than stoichiometric. Since the boiling point of CH_3I is ~42°C, it is quite possible that an inefficient fractional distillation would result in a poor separation of the methyl iodide contaminant from the trimethyl gallium (B.P. ~55°C). Such inefficient fractionations would result if the purification was done with Hempel, Vigreaux, or other nonadiabatic distillation columns. Such

columns do not have the necessary theoretical plate characteristics which are required for the impurity separations discussed here.

Table VI. Possible Synthetic Routes to TMGa-A Source Material

- Alkylation of magnesium/gallium alloy

$$6CH_3I + (Mg_3Ga_2)\ \text{Alloy} \xrightarrow{\ddot{O}} 3MgI_2 \downarrow + 2(CH_3)_3Ga$$

- Grignard alkylation of gallium tri-iodide

$$CH_3I + Mg \xrightarrow[I_2]{\ddot{O}} CH_3MgI\ \text{(ether complex)}$$

$$CH_3MgI\ \text{(ether complex)} + GaI_3 \xrightarrow{\ddot{O}} 3MgI_2 \downarrow + (CH_3)_3Ga$$

- Redox alkylation of gallium mono-iodide

$$2CH_3Li + GaI + CH_3I \xrightarrow{\ddot{O}} (CH_3)_3Ga + 2LiI \downarrow$$

The origin of the low molecular weight hydrocarbons in the as-received TMGa-A source material is unknown. It is possible that the apparatus used to synthesize the TMGa and/or contain the final product for shipment was decreased with hydrocarbon solvents. Inefficient thermal vacuum out-gassing of this equipment could certainly lead to such contamination of the metal alkyl. Moisture on the surface of the synthesis apparatus and/or containment bubblers could easily account for the methane found:

$$R_3M + HOH \longrightarrow R\text{-}H\uparrow + R_2M\text{-}OH \quad (3)$$

$$R\text{-}MgI + HOH \longrightarrow R\text{-}H\uparrow + Mg(OH)I \quad (4)$$

$$R\text{-}Li - HOH \longrightarrow R\text{-}H\uparrow + LiOH \quad (5)$$

$R = CH_3$
$M = Ga$

The trace amount of CH_3OH found in the TMGa-B source material could not be present as a contaminant owing to its immediate reaction with TMGa as follows:

$$CH_3OH + (CH_3)_3Ga \rightarrow CH_4 + (CH_3)_2GaOH \quad (6)$$

It most likely is generated by surface reactions of $CH_3\cdot$ in the mass spectrometer.

2.5.2 Repurification of TMGa-A Source Material

The quartz distillation apparatus was first passivated according to the technique described earlier, and the quartz still pot subsequently charged with ~110 grams of TMGa-A by a gravity-feed process. After equilibrating the apparatus for several hours at ~55.47°C (head temperature), the fractionation was commenced. Three major fractions of colorless TMGa liquid were collected in bubblers over a period of ~240 minutes: the first, ~34 grams over a temperature range of 55.47°C-55.64°C; the second, ~40 grams over a temperature range of 55.67-56.32°C; and the third, over an interval of 56.37°C-57.80°C. Vacuum distillation of the residuals in the column and still pot left a yellow-brown viscous oily residue at the bottom of the still pot. Pumping on this oil for ~2 days through a -50°C bath into a -196°C trap in series condensed an oil of low volatility at -50°C, and left a brown-yellow residue in the pot.

Fraction #2 of repurified TMGa-A was characterized by the MOCVD use test and mass spectroscopy. The involatile pot residue was analyzed by mass spectroscopy and emission spectroscopy; the -50°C bath material was analyzed by mass spectroscopy. An emission spectrographic analysis was performed on the white solid which was formed at the safety bubbler exit from the hydrolysis/oxidation of TMGa vapors carried there in the argon blanket gas.

2.5.3 Repurification of TMGa-B Source Material

The high purity TMGa-B material was redistilled in a recleaned, reassembled, and repassivated quartz distillation apparatus. The still pot was charged with ~83 grams of TMGa-B. The liquid was canary yellow in color. After equilibrating the apparatus for several hours at ~55.61°C (head temperature), the fractionation was commenced. Three major fractions of colorless TMGa liquid were collected in bubblers over a period of 405 minutes: the first, ~28 grams over a temperature range of 55.61°C-55.64°C; the second, ~40 grams from 55.64°C-55.68°C; and a third, ~10 grams over an interval of 55.68°C-55.71°C. Vacuum distillation of the residuals in the column and still pot left a light colored (white/yellow) solid. Pumping on this solid for ~2 days through a -50°C bath into a -196°C trap in series did not change the appearance of the pot residue but condensed a colorless material of low volatility at -50°C.

Fraction #2 of repurified TMGa-B was characterized by the MOCVD use test and mass spectroscopy. The involatile pot residue was examined by emission spectroscopy. The -55°C bath material was analyzed by both mass and emission spectroscopy. The TMGa vapors which exited the distillation apparatus in the argon blanket gas formed a white solid (hydrolysis/oxidation product) which was characterized by emission spectroscopy.

2.5.4 Characterization of Repurified TMGa-A and TMGa-B Source Materials

The electrical transport properties of undoped GaAs films grown with the repurified TMGa sources are summarized in Table VII. The data indicate

that repurification of the TMGa-A via one distillation substantially improved the 77°K mobility of the films by a factor of about 3 and reduced the donor level by one order of magnitude. For films grown by APMOCVD, the total ionized impurity concentration was reduced by ~82%; for LPMOCVD, $(N_D + N_A)$ was reduced by ~72%. It is not clear why the transport properties of films grown by LPMOCVD are slightly inferior to those grown by APMOCVD.

Table VII. Electrical Properties of GaAs Grown by MOCVD With Purified Trimethylgallium Source Materials

Property	Source A		Source-B	
Mobility at 77°K[a]	76,232	64,923	68,439	105,582
$(N_D - N_A)$ at 77°K	3.8×10^{14}	3.9×10^{14}	5.5×10^{13}	2.1×10^{14}
$(N_D + N_A)$ at 77°K	1.3×10^{15}	1.8×10^{15}	1.6×10^{15}	2.8×10^{14}
$AsH_3/(CH_3)_3Ga$	~40/1	~103/1	~40/1	~103/1
Technique	APMOCVD	LPMOCVD	APMOCVD	LPMOCVD

[a] film thickness for all samples ~20 μm

The repurification of the TMGa-B via one distillation did not seem to introduce additional major contaminants into the material nor did it appear to remove any since the electrical properties of the films grown were essentially the same as those previously obtained with the same sources.

Far infrared photoconductivity experiments performed on films grown with MOCVD-A sources before and after repurification are summarized in Fig. 8. Carbon is observed to be the dominant donor impurity in films grown before and after distillation, but it appears to be present to a lesser extent in films grown with repurified TMGa-A. As a result of the distillation, impurities such as tin and silicon in the GaAs films became more evident. This is due in part by limitations in the technique for measuring materials with electron mobilities at 77°K less than ~60,000 $cm^2/V\text{-sec}$.

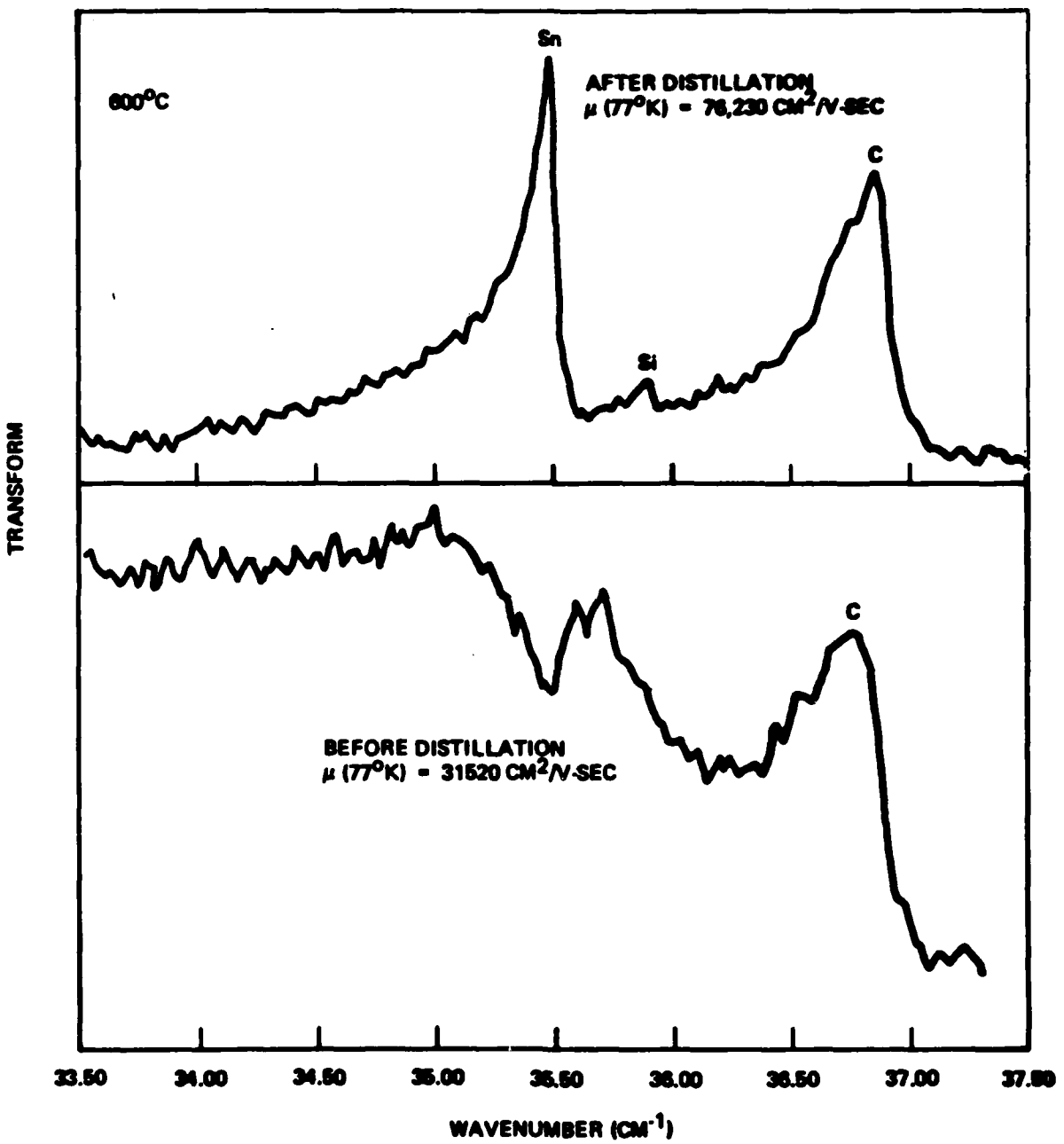

Fig. 8 Photoconductivity spectra of GaAs grown Labolac TMGa before and after distillation.

A more dramatic indication of the effect of the distillation on residual donors in the undoped gallium arsenide films can be seen from Fig. 9, which summarizes the far infrared photoconducivity results for GaAs grown with TMGa-B before and after repurification. Carbon is again the dominant impurity, but its presence is significantly reduced as a result of the distillation. The silicon and unidentified X_1 impurities are also seen to be present to a much lesser extent in films grown with repurified TMGa-B.

Spectrometric analyses of the pot residues are presented in Table VIII. These data indicate that tin is a significant impurity in the particular batch

Table VIII. Spectrometric Analyses of Pot Residues

TMGa-A Repurification		TMGa-B Repurification	
Mass Spectrometric (Qualitative)	Emission Spectrometric (Weight %)		Emission Spectrometric (Weight %)
CH_3I	Ga	74%	Ga 47%
	Sn	0.011	Sn <0.006 (ND)
$(CH_3)_3Ga$	B	<0.004 (ND)	As 2.6
	Si	0.035	Si 15
$R_1-\ddot{O}-R_2$	Mg	0.0029	Mg 0.0025
	Fe	0.0038	Fe 0.46
	Co	0.00056	Al 0.20
	Ag	<0.0001 (ND)	Cu 0.0072
	Ni	<0.001 (ND)	Ag <0.003 (ND)
	Ca	0.0024	Ni 0.069
	Cr	<0.0002 (ND)	Ca 0.0036
	Al	0.0038	Cr 0.024
			Ti 0.0062
			Mn 0.11

(ND) This element was not detected; the limit of detection for this analysis was less than the amount stated in the table above.

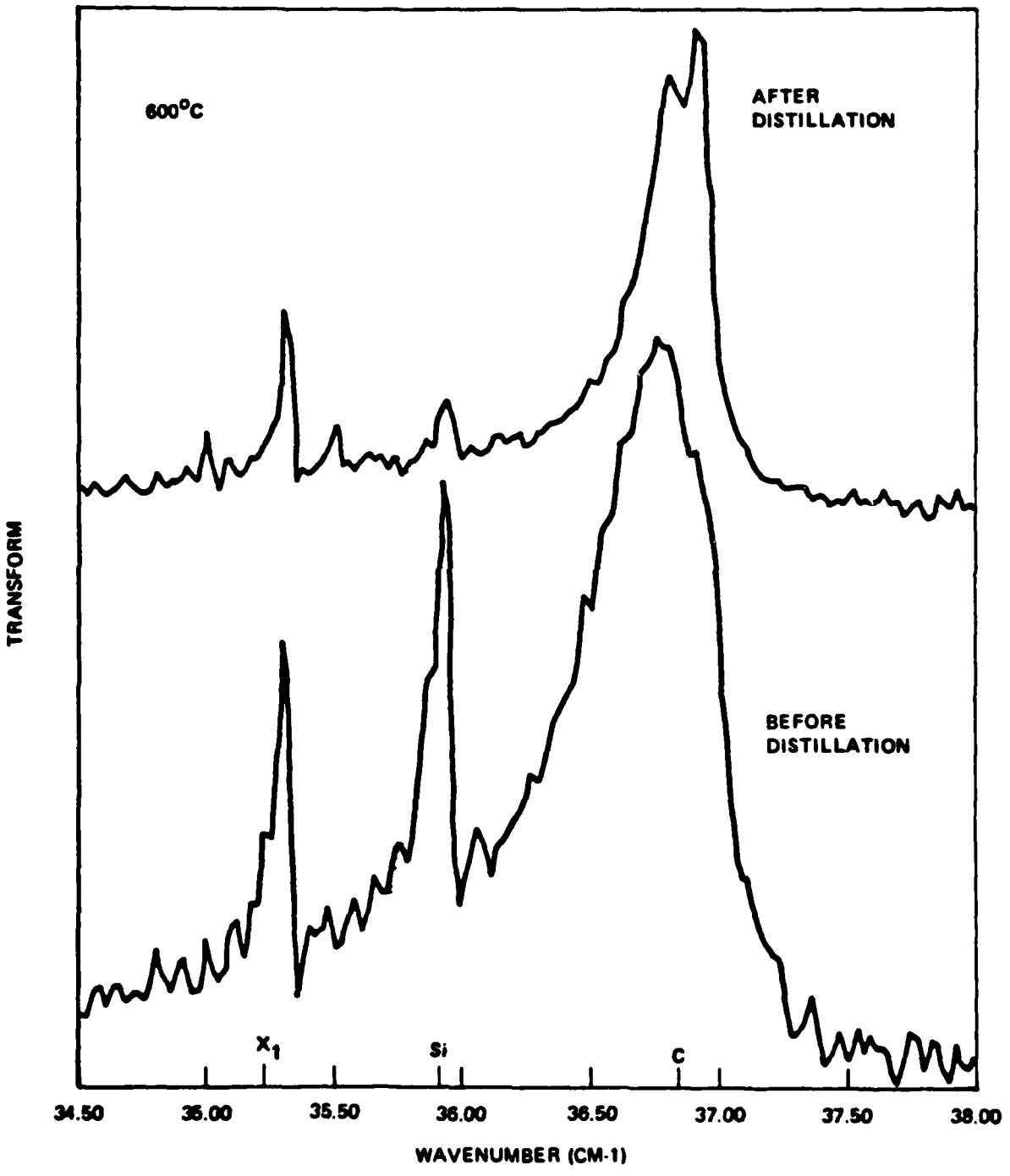

Fig. 9 Photoconductivity spectra of GaAs grown with Texas alkyl TMGa before and after distillation.

of TMGa-A evaluated and provides complimentary evidence to the far infrared photoconductivity measurements discussed earlier. The very high silicon content found in the TMGa-B pot residue suggests that the distillation process concentrated this particular contaminant in the pot and is partly responsible for the significant reduction of silicon in GaAs films grown with repurified TMGa-B as previously determined by the far infrared photoconductivity measurements.

The presence of arsenic in the TMGa-B residue is not difficult to understand if one considers the fact that the source bubbler had been used for ~24 months in the GaAs MOCVD growth apparatus prior to the repurification experiment. The exit of the bubbler was directly interfaced with the mixing manifold of the reactor. Since very low flows of H_2 passed through the bubbler (10-15 ccpm), it seems reasonable to expect some back diffusion of AsH_3 into the bubbler with subsequent formation of a less volatile addition complex, perhaps $ASH_3 \rightarrow (CH_3)_3Ga$. Such a material would tend to concentrate in the still pot during the low temperature distillation and eventually manifest itself as one of the involatile components of the residue.

The lack of any such arsenic in the TMGa-A residue is probably due to the limited number of MOCVD experiments performed with that particular bubbler.

A key to the possible synthetic history of TMGa-B is provided by the high concentration of aluminum in the TMGa-B residue. The most probable synthetic route based on this analysis would be as follows:

$$3(CH_3)_3Al + GaCl_3 + 3KCl \xrightarrow{\Delta} (CH_3)_3Ga + 3K[(CH_3)_2AlCl_2] \qquad (7)$$

The presence of ether linkage (R_1-$\ddot{O}$-R_2) and CH_3I in the TMGa-A residue lends further support to the synthetic history of TMGa-A proposed in Table VI. It remains to be determined how much a commercial vendor of TMGa will be willing to reveal about his synthetic process without jeopardizing his competitive position in the market place.

The presence of significant amounts of Mn, Fe, Ni, and Cr in the TMGa-B residue suggests that these elements may have been chemically leached from the stainless steel bubbler used to contain the TMGa throughout the 24-month period prior to repurification. These particular elements are major components of Series 300 AISI austenitic stainless steels. The absence of Mn, Ni and Cr in the TMGA-A residue and presence of only ~0.0038 weight percent Fe reaffirms the belief that such leaching effects may be realized over extended time durations. The TMGa-A material was exposed to the stainless steel container environment for only a few short months.

All four of these metal microimpurities are first row transition metals and with the exception of manganese ($[Ar]3d^5 4S^2$) would be expected to utilize their d orbitals not to form ordinary shared-pair or σ bonds with TMGa, but to establish other electron-sharing symmetry schemes through hybridization which are closer to donor-acceptor bonds with $(CH_3)_3Ga$ than to ordinary covalent bonds, and to come in the realm of coordination chemistry during the leaching process.

Qualitative mass spectrometric analyses were performed on the repurified TMGa source materials, and the results are summarized in Table IX. The data indicate that after one fractional distillation, only trace amounts of CH_3I were present in TMGa-A. Methane and other low molecular weight hydrocarbons were still present in about the same relative concentration levels as originally found in the TMGa-A source material. This suggests that the number of theoretical plates required to separate these carbon contaminants from TMGa is greater than that characteristic of the packed column used in this study. It seems likely that the use of a spinning band column would help correct this separation problem due to the larger diffusion coefficient of the vapor which results from the turbulence created by rotation of the band.

Originally, it was thought that the unidentified m/e-104 and m/e-73 peaks came from the compound trimethylsilyl methyl ether, $(CH_3)_3\ SiOCH_3$. However, close examination of the mass spectrum indicated that the characteristic fragmentation pattern on the trimethylsilyl group, $(CH_3)_3Si$, was

absent. This group breaks to give a large peak at m/e-58 due to loss of one of the methyl groups from the highly branched silicon atom, and this is always the largest peak in this heavy ion group and would have been the base peak in the spectrum. The mass spectrum of such a silicone contaminant would also be expected to give very large re-arrangement peaks at m/e-31, m/e-45, m/e-59 with formulae $(SiH_3)^+$, $(SiCH_3H_2)^+$, and $[Si(CH_3)_2H]^+$ which are formed from the $Si(CH_3)_3$ end of the molecule by elimination of methyl groups with replacement of a single hydrogen atom for every methyl lost. A series of peaks would also have been expected at m/e-47, m/e-61, and m/e-75 formed by the addition of the oxygen atom to the above ions. The characteristic isotope abundances for the heavy isotopes of silicon (Si^{28}, 92.2%; Si^{29}, 4.7%; Si^{30}, 3.1%) were also absent. The detected absence of any volatile silicon compounds in the repurified TMGa material seems to suggest that any contaminating reactions

Table IX. Qualitative Mass Spectrometric Analyses of Repurified TMGa Source Materials

Required TMGa-A Gas Phase Composition	Repurified TMGa-B Gas Phase Composition
$(CH_3)_3Ga$	$(CH_3)_3Ga$
Trace CH_3I	CH_3OH
CH_4	CH_4
C_NH_{2N+2}, C_NH_{2N} ; $N < 5$	H_2
H_2	Unidentified m/e-73
CH_3OH	Unidentified m/e-104

between $(CH_3)_3Ga$ and the SiO_2 network are minimal and that high purity quartz serves as a suitable agent in which purifications can be done. Such contaminating reactions might include the following:

TMGa + QUARTZ ⟶

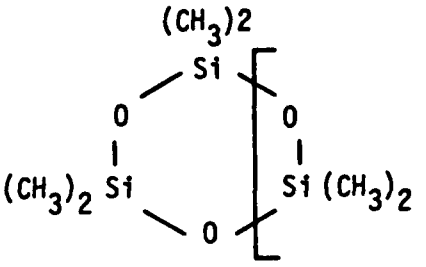

n $n = 0, 1, 2, 3$

CYCLIC POLYMER

TMGa + QUARTZ ⟶

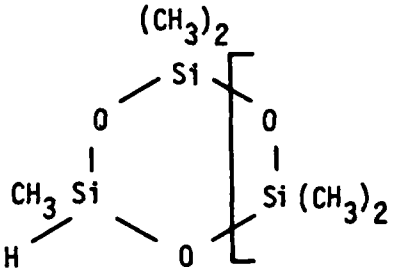

n $n = 0, 1, 2, 3$

LINEAR POLYMER

$$\text{TMGa + Quartz} \longrightarrow (CH_3)_3Si[OSi(CH_3)_2]_N \qquad n = 0,1,2,3$$

$$\text{TMGa + Quartz} \longrightarrow (CH_3)_4Si$$

$$\text{TMGa + Quartz} \longrightarrow (CH_3)_3SiOR$$

Mass spectrometric analysis of the TMGa-A column hold-up material (trapped at -55°C) showed the presence of an ether R_1OR_2 in addition to undistilled TMGa-A. A corresponding analysis of the TMGa-B column hold-up material (-55°C bath) indicated that nitropropane, $NO_2(CH_2)_2CH_3$, was present

as a contaminant. Nitropropane is a commonly used industrial solvent and could have been used to clean the TMGa-B source bubbler prior to filling. Its boiling point of ~132°C dictates its concentration in the column hold-up and subsequent isolation during vacuum distillation at -55°C.

An emission analysis was also performed on the -55°C trap material, and the results summarized in Table X. The extremely large decrease in the amount of silicon found in the -55°C trap residue (~0.31 wt.%) compared to that detected in the pot residue (~15 wt.%) indicates that the silicon contaminant is basically nonvolatile. The presence of ~1 wt.% Al adds more support to the previous proposal that an aluminum alkyl, i.e., TMAl, was

Table X. TMGa-B -55°C Bath Material Emission Analysis

Emission Spectrometric (weight percent)	
Ga	19%
Si	0.31
Al	0.84
As	Trace <0.03
B	0.0022
Mg	0.0089
Mn	0.00067
Fe	0.036
Cr	0.00025
Ni	0.0085
Sn	Trace <0.001
Cu	0.00098
Ag	0.00041
Ti	0.00062
Ca	0.068

probably used in the synthesis of TMGa-B. As would be expected, the concentration of major transition metal microimpurities Fe, Ni, Cr, and Mn is quite small (as compared to that found in the TMGa-B pot residue) presumably due to the absence of delocalized electron ligands which would impart more volatility to these metal contaminants.

Table XI summarizes the emission spectrographic data for TMGa-A and TMGa-B vapors which were hydrolyzed/oxidized at the exit to the distillation apparatus during the repurification process. No particular significance should be attached to these analyses. Because of the different conditions under which each purification was performed, the data merely establishes the

Table XI. TMGa-A and TMGa-B Hydrolysis/Oxidation Product Emission Spectrometric Analysis

TMGa-A Emission Spectrometric (Weight percent)		TMGa-B Emission Spectrometric (Weight percent)	
Ga	74%	Ga	74%
Sn	<0.004 (ND)	Sn	<0.002 (ND)
B	0.012	B	0.0061
Si	0.15	Si	0.088
Mg	0.0017	Mg	0.00065
Fe	0.0078	Fe	0.0017
Al	0.038	Al	0.013
Cu	0.00015	cu	0.00015
Ag	0.00025	Ag	<0.0001 (ND)
Ni	Trace <0.01	Ni	<0.0005 (ND)
Co	0.0018	Ti	<0.001 (ND)
Ca	0.0042	Ca	0.0019
Cr	0.0021	Cr	<0.0002
		As	<0.08 (ND)
		Mn	<0.001 (ND)

presence of these microimpurities (ppm range) in the gas phase during the distillation of TMGa source materials, and that elimination of them would require very sophisticated techniques, such as that used during the laser repurification of silane.

2.5.5 Characterization of Arsine Source Material

A sample of arsine/hydrogen used during this study was analyzed by mass spectroscopy and gas chromatography for gas composition. The results are summarized in Table XII. The gas composition agreed with the vendor's analysis. A more complete emission spectrometric analysis of this material resulting from its pyrolysis in a quartz chamber will be reported at a later date.

Table XII. Analysis of Arsine/Hydrogen Source Materials

Constituent	Mole Percent
H_2	89.261
H_2O	0.000
N_2	0.000
O_2	0.002
Ar	0.001
CO_2	0.000
AsH_3	10.736
Hydrocarbons	ND < 1 ppm Total

2.5.6 Evaluation of TMGa-B With Specially Prepared Arsine/Hydrogen Source Material

Arrangements were made with the vendor of AsH_3-In-H_2 materials to prepare three different cylinders of AsH_3/H_2 from the same AsH_3 synthesis, the cylinders to represent a head, middle, and tail fraction of the pure AsH_3. Analysis was then made of the light organic compounds of each AsH_3 fraction in its cylinder before mixing with UHP-H_2 and subsequent analysis of the mix-

ture. The results are summarized in Table XIII. The "inferiority" of the head fraction was demonstrated when undoped films were grown with 77°K mobilities of only $\mu_{77} \approx 50{,}000$ $cm^2/V\text{-sec}$ with a net carrier concentration of $(N_D - N_A) \approx 1.8 \times 10^{15}$ cm^{-3}. The middle fraction led to films with $(N_D - N_A) \approx 1.5\text{-}3.5 \times 10^{14}$ cm^{-3} and $\mu_{77} \approx 70{,}000$ $cm^2/V\text{-sec}$.

Table XIII. Compositional Analyses of Special Prepared AsH_3/H_2 Mixtures

Components	Concentration		
	Head	Middle	Tail
AsH_3 (99.9995%)	10.09%	10.0%	9.98%
N_2	<1 ppm	<1 ppm	<1 ppm
O_2	<1 ppm	<1 ppm	<1 ppm
Ar	<1 ppm	<1 ppm	<1 ppm
CH_4	<1 ppm	<1 ppm	<1 ppm
CO	<1 ppm	<1 ppm	<1 ppm
CO_2	<1 ppm	<1 ppm	<1 ppm
H_2 (99.9999%)	Balance	Balance	Balance
Light Organic Analysis[a]			
CH_4	0.06 ppm	0.05 ppm	ND <0.003 ppm
C_2H_4 and/or C_2H_2	0.06 ppm	0.02 ppm	0.01 ppm
C_2H_6	0.02 ppm	0.02 ppm	0.01 ppm
C_4's	ND <0.04 ppm	ND <0.04 ppm	0.04 ppm
C_5's	ND <0.04 ppm	ND <0.04 ppm	0.04 ppm

[a] Organic analysis of the pure AsH_3 after its transfer to the individual mixture cylinders and before addition of the UHP-H_2.

The optimized electrical transport properties were realized when undoped GaAs films were grown using the tail fraction of AsH_3/H_2. The results

are summarized in Table XIV. These results attest to the high quality AsH_3-In-H_2 in this tail fraction and indicate the value of fractionating the AsH_3 as well as the TMGa when extremely high purity layers are needed for specific device fabrication.

Table XIV. High Purity GaAs Grown by MOCVD with Repurified TMGa-B and Tail Fraction AsH_3

Property	LPMOCVD	APMOCVD
Mobility at 77°K	125,220	103,775
$(N_D - N_A)$ at 77°K	4.8×10^{13}	1.1×10^{11}
$(N_D + N_A)$ at 77°K	$<6 \times 10^{13}$	3.5×10^{14}
$AsH_3/(CH_3)_3Ga$	103/1	40/1

3.0 CONCLUSIONS

Several important demonstrations were achieved in this program that result in a new assessment of the suitability of MOCVD for the growth of GaAs for microwave devices. These are:

1. Growth of high purity GaAs with commercially available sources.
2. Identification of the dominant residual impurities in MOCVD GaAs.
3. Demonstration of the improvement of film properties by reduced pressure growth.
4. Demonstration of the improvement of film properties after repurification of TMGa.
5. Illucidation of techniques for repurifying TMGa.
6. Demonstration of the highest purity GaAs grown with TMGa and arsine ($N_D + N_A$) $< 5 \times 10^{14}$).

These demonstrations lead to the conclusion that MOCVD is suitable for the growth of GaAs for microwave devices provided that one is careful in the selection of source materials. There are no inherent impurity species which prevent the attainment of device quality material although carbon will probably limit the 77°K mobilities to near the best values obtained in this program. Even with less than pure commercial TMGa, high purity can be achieved with relatively simple repurification by distillation. It is believed that the ultimate purity of MOCVD GaAs has not yet been achieved. The major growth parameter controlling the purity of the grown material is the growth temperature. In this program we were unable to grow at temperatures below 575°C despite the continuing improvement in purity observed as the growth temperature was decreased. This resulted from the reduction in the effective As concentration at the growth interface owing to incomplete pyrolysis of the arsine. Techniques for further reducing the growth temperature and maintaining the required As overpressure will undoubtedly result in lower impurity incorporation.

4.0 RECOMMENDATIONS

The work performed in this program has clearly indicated the potential of MOCVD growth in the fabrication of microwave devices. Only a demonstration is now required to realize this potential.

More reproducible yield of high purity GaAs could be achieved by investment in cleaner synthesis and materials handling techniques.

Further improvement in the purity and perhaps the yield of high purity GaAs by MOCVD may be achievable by growth at lower temperatures. Arsenic sources that allow growth at lower temperatures such as elemental arsenic and perhaps TMGa are candidates for study.

These considerations lead to the following recommendations for further study:

1. Investigate the performance of GaAs microwave devices using MOCVD as the growth technique for the epitaxial layers.
2. Investigate higher purity techniques for synthesis and handling of TMGa and arsine.
3. Investigate other sources of arsenic for MOCVD growth to allow growth at lower temperatures.
4. Investigate techniques for incorporating high purity GaAs into superlattices (SL) and multiple quantum well (MQW) heterostructures.
5. Investigate the extension of techniques developed here to the growth of high purity GaAlAs for incorporation into SL's and MQW's.
6. Investigate the extension of the techniques developed here to other materials with potential for producing improved microwave devices such as GaInAs, GaInAlAs and GaInAsP.

APPENDIX I

High Purity GaAs Prepared from Trimethylgallium and Arsine (invited)

HIGH PURITY GaAs PREPARED FROM TRIMETHYLGALLIUM AND ARSINE (INVITED)*

P. D. Dapkus, H. M. Manasevit, and K. L. Hess
Microelectronics Research and Development Center
Rockwell International, Thousand Oaks, CA 91360, USA

and

T. S. Low and G. E. Stillman
Department of Electrical Engineering
University of Illinois, Urbana, IL 61801, USA

ABSTRACT

A study of the sources and control of residual impurities in CaAs grown by metalorganic chemical vapor deposition (MOCVD) is presented. The effects of source purity, growth temperature, and reactor pressure upon residual impurities incorporation are detailed. Far infrared photoconductivity and photoluminescence indicate that C, Si, and Zn are the dominant residual impurities in undoped material. It is demonstrated that GaAs with total impurity concentrations as low as 5×10^{14} cm^{-3}, μ (77°K) = 125,000 cm^2/Vsec, can be grown by MOCVD. The conditions for growing such material are detailed.

* This work was supported in part by the Naval Research Laboratory through Contract No. N00173-80-C-0066.

I. INTRODUCTION

Since the first demonstration of the growth of GaAs by metalorganic chemical vapor deposition (MOCVD) (1), a disturbing lingering question has been the source of the residual impurities and the limits on the purity ultimately to be obtained in material grown by this technique (1-4). Some of the early work in this field was hampered by the unavailability of high purity starting materials and incomplete understanding of the basic reaction mechanisms occurring during crystal growth. This question persists despite the achievement of very high performance devices using MOCVD, including solar cells (5), lasers (6-8), quantum well heterostructures (9), photocathodes (10), and FET's (11), over the past several years. Although vendors of starting materials have become more consistent in their product, lot-to-lot variations still plague attempts to obtain high purity material. The goal of this work is to identify the sources of the residual impurities in undoped GaAs grown with trimethylgallium (TMGa) and arsine (AsH_3), and to determine, if possible, the limits to the purity obtainable by the use of MOCVD growth technique.

Early workers in the field typically achieved purities in undoped material that were limited by the purity of the starting materials. Mobilities in the range of 10,000 to 20,000 $cm^2/Vsec$ at 77°K were typical for undoped GaAs grown over a range of temperatures from 650° to 750°K (1-2). Although little in the way of systematic variation of growth parameters or starting material purity were reported, many workers studied in some detail the characteristics of the resultant undoped material as well as the incorporation of both n- and p-type dopants into GaAs grown by MOCVD (12). Trimethylgallium has been the

most persistently used source for MOCVD because of its reasonably high room temperature vapor pressure which allows growth rates over a range 0.01 μm/min to 1 μm/min. A notable exception to this trend was work performed by Seki and co-workers. (4) In this work, triethylgallium was substituted for trimethylgallium, with the result that high purity GaAs (μ(77°K) = 120,000 cm^2/Vsec) was grown for the first time by MOCVD. It is not clear from the text of this work whether the high purity resulted merely from the use of triethylgallium of from improvements in the purity of the starting material.

More recently with the availability of better starting materials, some workers have concentrated on the elimination of source purity variations by selection of source materials and the reduction of specific residual impurities, especially C and O, by modifying the growth process. (13-14)

The work of Duchemin and co-workers (15-17) has focussed on MOCVD growth at reduced pressures. No systematic study of residual impurity incorporation by this process has been reported. However, the prospect of achieving lower temperature growth and modifying the characteristics of the stagnant boundary layer by varying the pressure, present new tools for controlling and understanding residual impurity incorporation of MOCVD grown GaAs.

In this paper, we will compare the properties of undoped GaAs grown at atmospheric pressure and at reduced pressure utilizing a variety of source materials. Detailed characterization of the transport properties of materials grown under these conditions as well as the

determination of the specific residual donor species in the material will be reported and discussed. In addition, preliminary results on the residual acceptor species as determined by low temperature photoluminescence will also be reported. From these data, we will determine the optimum conditions for the growth of high purity GaAs by MOCVD, identify some of the sources and impurities in GaAs grown by MOCVD, and discuss the limitations on the purity of GaAs achievable by this growth technique.

Section II of this paper describes the experimental procedures used in this work. Section III details the experimental results achieved for atmospheric pressure growth, and Section IV describes similar results for reduced pressure growth. In Section V, we discuss and compare these results, and conclusions are reached about the sources of impurities in MOCVD-grown GaAs.

II. EXPERIMENTAL PROCEDURES

A. Reactor Design

The growth reactor used in these studies is a modification of the standard vertical growth reactor used in our previous studies (see Fig. 1). The reactor gas manifold and mixing system are constructed totally of stainless steel. Electronic mass flow controllers are employed for control of the various gas flow rates and pneumatically controlled bellows valves for the switching of all gaseous species. The AsH_3 is contained in commercially supplied high pressure gas cylinders. Both the AsH_3 and the ultra high purity, palladium-purified H_2 are passed through a -50°C cold trap before entrance

into the gas manifold system to remove residual water vapor. The trimethylgallium is contained in specially prepared stainless steel bubblers that have been thoroughly cleaned and passivated. A unique aspect of this reactor is that there are no dopant gases included in the reactor system. It has been used exclusively for the growth of undoped GaAs and for the studies to be reported in this paper. The reactor is also constructed to include two source ports for trimethylgallium. A consistent procedure used in this program has been to evaluate a source of trimethylgallium and AsH_3 utilizing the "less pure" trimethylgallium port before introducing it into the highest purity portions of the reactor. The cold walled growth vessel is a quartz cylinder with O-ring seals for separation at the base, and the reactor gas manifold is coupled to the vessel with Ultra-torr fittings. A silicon carbide coated graphite susceptor is RF inductively heated. The system is constructed to accommodate up to 2" diameter GaAs wafers.

Growth at reduced pressures is accommodated by incorporating a high capacity (17 CF/M) Alcatel chemical resistant pump at the outlet of the reactor vessel. Equipment to monitor the pressure within the vessel and within the gas manifold are also incorporated into the design.

B. Growth Procedures

Substrates used in the growth studies of this paper are all chemically mechanically polished prior to incorporation into the reactor. Each substrate is thoroughly degreased and cleaned and given a brief 1:1:10 H_2O_2:H_2SO_4:H_2O etch to remove surface oxides and residual

contamination. Prior to the initiation of growth and after the temperature of the susceptor reaches 500°C, AsH_3 flow is initiated and maintained when the temperature is above 500°C. Once the desired temperature is reached, trimethylgallium is introduced into the reactor to initiate growth. The growth rates are linearly dependent on the flow rate of trimethylgallium in the growth vessel.

For reduced pressure growth, the exit of the reactor is connected to the high capacity pump. Pressure within the reactor is controlled by throttling the input to the pump with high purity N_2 gas. The pressure within the gas mixing manifold is maintained slightly above atmospheric pressure by incorporation of a needle valve at the inlet to the reactor vessel. This allows the flow rate of TMGa to be controlled entirely by the hydrogen passed through the TMGa bubbler and reduces the possibility of cooling by surface evaporation. The temperature prior to growth is monitored by an optical pyrometer. No feedback control of the growth temperature is utilized in this system. At ± 5°C temperature stability has been observed during an entire growth run. Table I lists the optimum growth conditions for atmospheric pressure growth and reduced pressure growth that were determined during this study.

C. Electrical Characterization

The samples grown in this study were characterized using van der Pauw geometry Hall effect measurements and capacitance-voltage carrier concentration profiling. Van der Pauw measurements were performed on reactangular samples by contacting them with In dots around the periphery

of the sample. Care was taken to avoid edge leakage effects in higher resistivity samples. The Hall effect was measured in an automated Hall apparatus utilizing a 5 kG magnetic field. 77°K measurements were performed by immersing the sample in liquid nitrogen. Temperature dependent measurements were made in the same automated apparatus by heating the sample immersed in the vapors from liquid nitrogen. Carrier concentration profiling of several samples was performed on material grown on n^+ substrates by contacting the back of the substrate with AuGe:Ni:Au metallization and by depositing photolithographically defined Au Schottky barrier dots to the top surface of the sample. The measurements were performed on a Lehighton Miller feedback profiler.

D. Donor and Acceptor Spectroscopy

The residual donor species present in the undoped GaAs were identified by far infrared photoconductivity measurements (18-20). This technique is based upon the photo-thermal ionization of neutral donor species in GaAs. Donors in GaAs are known to be hydrogenic impurities. The ground state of each specific donor, however, is slightly modified by central cell effects specific to the particular impurity. Therefore, the energy between the ground state and the first excited state of each donor impurity is found to vary from donor to donor. These energies have been carefully cataloges by several workers (18-22), with the net result that identification of donors in GaAs can be achieved provided that the concentration of donors and acceptors is low enough to avoid smearing of the transitions due to localized electric field effects and screening.

Implementation of far infrared photoconductivity for donor spectroscopy is carried out by immersing a sample cooled to liquid helium temperatures in a magnetic field such that the transition between the ground state and various excited states are split owing to the Zeeman effect. A tunable far infrared light source is then directed on the sample, and the change in the conductivity as a function of the wavelength of the tunable source is measured. At 4°K, there are many phonons with sufficient energy to thermally excite an electron from an excited state of the donor into the conduction band, but few with sufficient energy to excite an electron from the ground state to the conduction band. As a result, the extrinsic photoconductivity shows a series of peaks owing to transitions from the ground state to the various excited states. By concentrating on one of these transitions, namely the 1 s to 2 p (m = -1) transition, high resolution photoconductivity measurements can identify transitions occurring on different donor species within the material. If the doping is sufficiently low, these transitions are sharp, and the donor species can be clearly identified. The data to be presented in this paper were accumulated utilizing a magnetic field of 65 kG. The wave number for the 1 s to 2 p (m = -1) transitions of various donor species are shown in Table II. These peak identifications are based on previous work by Stillman and co-workers. (18-20) Though some of these identifications may be viewed as tentative, the majority are well accepted, and in cases where a controversy exists, the data presented in this paper may help clarify their identification. Figure 2 shows a schematic diagram of the photo-thermal ionization process utilized in the far infrared

photoconductivity measurements as well as the photoconductivity spectra of a sample with and without a magnetic field present. It is the 1 s to 2 p ($m = -1$) transition that is studied in detail in this paper to determine the specific donor species.

Low temperature photoluminescence to determine acceptor species (23) in GaAs was performed by immersing samples in liquid helium and illuminating them with the 5146 Å line of an argon ion laser. Care was taken to avoid saturation and heating effects in the excitation.

III. EXPERIMENTAL RESULTS -- ATMOSPHERIC PRESSURE GROWTH

The general characteristics of undoped GaAs grown by MOCVD at atmospheric pressure will be described in this section. Emphasis will be placed on the effect of the As to Ga ratio on the net carrier concentration of undoped GaAs, the temperature dependence of the total impurity concentration in undoped GaAs, and the effects of source purity on the total impurity concentration.

A. Effect of AsH_3/TMGa

A primary means of characterizing the undoped GaAs films grown in this program is the low temperature (77°K) mobility, μ_{77}. This can be correlated directly with the total impurity concentration in the material. (24) In order to accurately characterize the total impurity concentration by this means, it is necessary to have n-type conductivity. The AsH_3/TMGa ratio plays a major role in determining conductivity type in MOCVD growth. Figure 3 shows the variation with AsH_3/TMGa of the net carrier concentration ($N_D - N_A$) of undoped GaAs films grown at a variety of temperatures. The AsH_3 and TMGa used to generate these data were

amongst the purest starting materials examined in this study. Notice that at large values of AsH_3/TMGa, undoped material is predominantly n type with a carrier concentration in the range of low to mid 10^{14} cm^{-3}. As AsH_3/TMGa is decreased, the net carrier concentration of the material decreased until at AsH_3/TMGa ≈20, the material changes conductivity type and becomes p type. With decreasing AsH_3/TMGa below this point, the material becomes increasingly p type reaching a carrier concentration as high as 5×10^{15} cm^{-3}. The data presented in this figure is characteristic of growth by MOCVD. The exact ratio of AsH_3/TMGa at which the crossover from n- to p-type conductivity occurs depends upon the temperature of growth, growth rate, and the purity of the source materials. For relatively pure material used in this study, the crossover is insensitive to growth temperature and growth rate. For AsH_3/TMGa >30, the resultant epitaxial film is quite smooth showing only hillocks which decorate dislocations in the substrate. On the other hand, for very low Ga to arsine ratios (on the order of 10 to 15), the surface morphology of the film becomes quite rough. Behavior of this type serves as a yardstick to measure the effective AsH_3/TMGa in the vicinity of the substrate under quite different growth conditions, e.g., reduced pressure. At all times in this program the films which are characterized for total impurity concentration were grown under arsenic-rich conditions. Not only does this allow a comparison of the low temperature mobility to a well characterized model, but it also avoids the problem of attempting to measure the mobility of films which are totally depleted as would be the case of material grown near the crossover point. It also removes

the possibility of having regions of p-type conductivity imbedded in the film, a phenomenon that can sometimes occur near the crossover point. As will be seen in the next section, the point at which the crossover occurs at reduced pressure varies substantially from that observed at atmospheric pressure for these same sources of material.

B. Effect of Film Thickness on Mobility

Early workers attempting to grow high purity GaAs observed that the apparent mobility depended quite strongly on the thickness of film grown in the semi-insulating substrate (25). To examine this dependence for MOCVD growth, a series of films were grown of various thicknesses under identical conditions. These conditions were chosen to yield the highest μ_{77} under optimum growth conditions. Figure 4 shows the dependence of the film of μ_{77} on film thickness for these samples. The μ_{77} of the n-doped GaAs films is seen to increase rapidly with increasing film thickness reaching its maximum value at a thickness of about 20 to 25 μm. The cause for this change in apparent properties with film thickness is not completely understood. However, it is felt that the presence of substantial depletion layers at both the substrate-film interface and the film-surface interface contribute to the decrease in mobility at small film thicknesses. Other possible causes insulating substate. No attempt has been made to correlate this phenomenon with preheat time durations. However, to avoid this experimental difficulty,

all of the films described in the subsequent part of this paper are grown to thicknesses exceeding 20 μm.

C. Temperature Dependence of Total Impurity Concentration in MOCVD Grown GaAs

Under arsenic rich growth conditions, the most important variable that effects the total impurity concentration in undoped GaAs films is the growth temperature. Figure 5 shows the dependence of the μ_{77} for undoped GaAs grown at atmospheric pressure upon the growth temperature for a series of films grown with the high purity starting materials. The mobility is seen to increase with decreasing growth temperature up to a growth temperature of approximately 600°C at which point the μ_{77} of the material is 87,000 $cm^2/Vsec$. At temperatures below 600°C, the mobility decreases rapidly falling to very low values at 550°C. We believe this falloff is due to incomplete pyrolysis of the AsH_3 and an effective reduction in As/Ga in the vicinity of the substrate. At these temperatures, the film becomes highly resistive and the morphology becomes rough and irregular--similar to conditions at higher growth temperatures under more Ga rich conditions. By utilizing these mobility values and the measured net carrier concentration at 77°K, we can determine the dependence of both the donor and the acceptor concentration as a function of temperature. This is plotted in Fig. 6 along with the total impurity concentration, $N_D + N_A$. Note that both the donor and acceptor concentration decrease with decreasing temperature. At temperatures of 600°C, the total impurity concentration is $10^{15}/cm^3$. More recent results with higher purity AsH_3 have resulted in

films grown under these conditions at 600°C with mobilities as high as 102,000 cm^2/Vsec.

D. Source Purity Effects

A major source of impurities in undoped GaAs by MOCVD is impurities in the starting source materials. The importance of the source purity is illustrated in Table III, where we have listed the range of μ_{77} observed with a variety of source materials under the conditions for optimum growth conditions as defined in the previous section. Note that ultimate purity of undoped GaAs grown by MOCVD depends very strongly on the particular source of TMGa and AsH_3 used in the growth. The highest purity source of TMGa that we were able to obtain during this study--source TA-1--yielded material with μ_{77} as high as 87,000 cm^2/Vsec used with two high purity AsH_3 sources, PR-1 and PR-4. On the other hand, when this same source of TMGa was used with three other bottles of AsH_3, the resultant GaAs had substantially lower purity. For example, with source SG-1, μ_{77} was only in the range 38,000 to 45,000. Note that sources PR-2 and PR-3 are the same vendor as sources PR-1 and PR-4, and yet the material is of substantially lower purity than the other two bottles. This clearly points out the variability of AsH_3 purity from bottle to bottle. In fact, source PR-3 was from the same lot as source PR-1.

Note also the very strong dependence of the material purity upon TMGa source. Substantially lower purity material was obtained in using source AV-1 and L-1 with high purity AsH_3 sources than when source TA-1 was used. Presumably this is due to impurities in TMGa sources AV-1 and L-1. On the other hand, it is not clear that the ultimate purity

obtainable was obtained using sources TA-1 and PR-1 and PR-4. After redistillation (26) source TA-1 produced essentially equivalent purity material with PR-4 as it did prior to repurification. On the other hand, when repurified TA-1 was used with yet another and even higher purity source of arsine PR-5, even higher purity material resulted. The mobility obtained with these latter two sources is the highest purity GaAs we have obtained under atmospheric pressure growth with TMGa and AsH_3.

E. Donor and Acceptor Spectroscopy

Selected samples of undoped material were examined by far infrared photoconductivity and low temperature photoluminescence to determine the specific donor and acceptor species incorporated in the material. Table IV shows the predominant species of impurities observed in GaAs grown at atmospheric pressure. The dominant acceptors observed in 4°K photoluminescence are carbon, silicon, and zinc. The dominant donor species are identified as carbon, silicon, and the X1 donor level. Figure 7 shows the far infrared photoconductivity spectra of three samples grown under atmospheric pressure conditions with high purity sources of TMGa (TA-1) and AsH_3 (PR-1) at three growth temperatures. Several features of these spectra are worthy of mention. First, there are three dominant donor peaks observed. These occur at energies identified with to the X1, silicon, and carbon donor $1s\text{-}2p^-$ transitions. In all cases, the peak associated with carbon dominates the spectrum. The X1 peak decreases in intensity with decreasing growth temperature. At 700°C, the peaks associated with the various donors are greatly broadened by local field variations

This results in a tailing of the threshold for the 1 s to 2 p^- transition on the low energy side. As the growth temperature is decreased, the purity of the material increases, resulting in less electric field interaction between impurities, and the spectra become much sharper. At 600°C growth temperature, the various peaks are well defined, but the X1 peak is absent from the spectra. The sample grown at 700°C represents about the lower limit of purity in which well resolved donor peaks can be observed. The identification of the donors given above is not universally accepted. For example, the peak associated here with carbon (21) has been identified in other work as being due to germanium. (22) However, Ge has not been detected in any analysis of TMGa or AsH_3 performed in this study. Furthermore, Ge is not observed as an acceptor in this material which it most certainly would be if incorporated in large enough quantities to be the dominant donor. Therefore, we contend that the donor transition identified here as being due to carbon is the result of carbon being incorporated on Ga sites as a donor.

IV. EXPERIMENTAL RESULTS--REDUCED PRESSURE GROWTH

Owing to the very strong temperature dependence of the mobility observed in atmospheric pressure MOCVD growth, an investigation of the growth of GaAs at reduced pressures was undertaken with the goal achieving even lower growth temperatures. The properties of the material were monitored in much the same way as atmospheric pressure samples, and films were grown at various temperatures under a variety of pressure conditions. In the present study, the pressure was varied from 1 atmosphere to 0.05 atmospheres. Experimental diffi-

culties related to the particular reactor configuration prevented investigation of growth at pressures lower than 0.05 atmospheres, and most of the results reported in this section were done under the conditions listed in Table I.

A. AsH_3/TMGa Effects

The growth of GaAs by MOCVD at reduced pressure requires certain modifications to the growth parameters in order to achieve n-type conductivity and high μ_{77}. Early investigations of growth at reduced pressure revealed that the occurrence of the crossover from n-type conductivity to p type occurred at much higher As to Ga ratios than occurred at atmospheric pressure. As the pressure was reduced, the apparent crossover occurred at even higher As to Ga ratios. This is believed to be caused by the reduction in the effective As overpressure near the substrate owing to a decrease in the effective pyrolysis of the AsH_3. As the pressure is reduced at a fixed flow rate, the velocity of the gases increases, and the interaction of the AsH_3 with the susceptor is minimized. The net result is that the effective concentration of As at the substrate-gas interface is substantially reduced. This is clearly shown in Table V where the mobility and carrier concentration for several films grown at 70 Torr and fixed AsH_3 flow rate are listed as a function of the As to Ga ratio in the gas stream. Note that in order to achieve n-type conductivity and in order to be able to measure high mobilities, it was necessary to cool the trimethylgallium to below 0°C. This effectively reduces the vapor pressure and decreases the flux of Ga delivered to the substrate. As shown in

Table IV, the As to Ga ratio conditions that are effective at room temperature to produce the high mobility n-type films now result in either high resistivity or p-type material. It was necessary to increase the As to Ga ratio to over 100 to achieve n-type conductivity and high mobilities. The reduction of TMGa flow was accompanied by a decreased growth rate (0.166 μm/min vs 0.055 μm/min). The major effect in changing the conductivity from p- to n-type, however, is the increased As to Ga ratio. Experiments carried out at atmospheric pressure show little dependence of the residual purity concentration in high purity GaAs upon the temperature of the TMGa and as a result the growth rate. Owing to the need to maintain much higher As to Ga ratios in the reactor to achieve n-type conductivity, all growths at reduced pressure were undertaken with the trimethylgallium cooled to -12°C or -20°C to reduce the vapor pressure of trimethylgallium.

B. Comparison of Atmospheric Pressure and Reduced Pressure MOCVD Growth

A major difference in the growth at reduced pressure compared to atmospheric pressure at low temperatures (600°C) is the considerably smoother morphology that results from reduced pressure growth. Figure 8 shows a photograph of two very thick (30 μm) GaAs films grown (a) at atmospheric pressure and (b) at reduced pressure. Note the smooth surface that results from reduced pressure growth while the atmospheric pressure growth results in hillocks over many regions of the sample surface.

The original motivation for investigating reduced pressure growth was the potential for achieving lower temperature epitaxial growth. In actual fact, owing to limitations in reactor system design, it was not possible to achieve growth at much lower temperatures (below 575°C) at reduced pressures. This resulted from the reduced pyrolysis of AsH_3 and the lower effective As overpressure at the substrate interface. At temperatures below 757°C, the films were either high resistivity of p-type with a very rough surface texture.

At the same growth temperature (600°C) consistently higher μ_{77} and sample purities were observed in reduced pressure growth as compared to atmospheric pressure growth. Table VI illustrates this consistent improvement in the μ_{77} showing the electrical properties of films grown under optimized conditions for atmospheric growth and reduced pressure growth with the same sources of AsH_3 and TMGa. In every case the μ_{77} of the sample grown at under reduced pressure conditions is equivalent or superior to that achieved under atmospheric conditions. The net carrier concentration at 77°K varies from sample to sample, and it is undoubtedly the result of a delicate balance between incorporation of donors and acceptors in the material. Note that the sample grown in run S-4 was measured to have a 77°K mobility of 125,220. This is the highest mobility we have measured for MOCVD grown GaAs and represents a total impurity concentration of approximately 5×10^{14} cm^{-3}.

C. Donor and Acceptor Spectroscopy

The low temperature photoluminescence characterization of material grown at reduced pressure indicates that the same three acceptors are

present in approximately the same ratios at reduced pressures as they are at atmospheric pressure. That is, carbon, silicon, and zinc appear to be present in equal quantities as acceptors in this material.

The far infrared photoconductivity examination of the donor species in material grown at reduced pressures similarly shows the presence of the same three donor levels as seen in atmospheric pressure. A major observed difference, however, can be seen in Fig. 9 where the photoconductivity spectra for two samples grown under reduced pressure conditions with different sources of TMGa and AsH_3. Notice that the ratio of the C to X1 donor peaks is substantially reduced as compared to the data of Fig. 7 at 600°C. This suggests that the carbon content of the film at reduced pressures is decreased.

V. DISCUSSION

A. Carbon Contamination

The data in this paper indicate that carbon is a dominant residual impurity in GaAs grown by MOCVD. Carbon is corporated both as a donor and as an acceptor under all conditions of growth examined. It is the dominant donor observed for all sources of TMGa and AsH_3 examined. The source of carbon is unknown. However, it may result from the fragmentation products of the metal alkyls used in the growth process. The very strong temperature dependence of both the mobility and the concentration of the carbon donors shown in Figs. 5 and 7, respectively, suggest that further reduction in the carbon content of MOCVD-grown GaAs can be achieved by lower temperature growth than has been attempted in this program.

Stringfellow and Hall (13) have predicted that growth by a modified MOCVD process including HCl will inhibit the incorporation of carbon in GaAlAs. The presence of the HCl results in clean cleavage of the Al-C bonds in trimethylaluminum and greatly inhibits carbon incorporation. It is possible that the inclusion of HCl in GaAs MOCVD growth would similarly reduce the carbon contamination. However, past experience with the use of HCl in MOCVD growth has indicated that HCl is by far the less pure reactant material.

B. Silicon Contamination

Silicon is also observed as an important residual impurity in the MOCVD GaAs films grown in this study. The occurrence of silicon contamination is not surprising, since silicon compounds are the predominant contamination observed in emission spectroscopy and mass spectroscopic analysis of trimethylgallium obtained from several sources. Recent studies on the redistillation of TMG (26) have indicated that the silicon compounds are persistent impurities though their concentration in the GaAs grown with redistilled material can be significantly reduced. The use of a cold-walled reaction system such as MOCVD should provide the advantage of reduced interaction with the growth vessel and reduced silicon contamination. However, the graphite susceptor is SiC coated and may be a source of Si. To effectively eliminate this impurity will require sophisticated TMGa distillation procedures and possibly other susceptor materials.

C. Other Impurities

The two other major impurities besides carbon and silicon observed in this study are zinc and an unknown impurity responsible for the peak labeled X1. The presence of zinc in the GaAs films is somewhat surprising, since

it was not detected as a metal impurity in any TMGa utilized in this program or in mass spectroscopic analysis of AsH_3. It is possible that it is introduced with the AsH_3 gas at the ppb level since Zn_2A_3 is used as the starting material in the synthesis of high purity AsH_3. A problem with zinc contamination is that the obvious trend to lower growth temperatures to reduce silicon and carbon contamination will result in enhanced incorporation of zinc (12,27).

The X1 donor observed in most of the samples examined to date has previously been related to a Ga vacancy complex (21) and to Si donors (22). It would appear that this donor can be effectively eliminated by growth under more Ga rich conditions (21). This inevitably occurs as the growth temperature is reduced. In fact, the data of Fig. 7 clearly show substantial reduction in the relative concentration of the X1 impurity level with decreasing growth temperature.

D. The Effects of Reduced Pressure Growth

The data presented in the previous sections show that a significant reduction of the residual impurity concentration (2 x lower) can be effected by growing at reduced pressures. For a given flow rate, the velocity of the gases increases inversely with the reactor pressure. This has the effect of reducing the residence time of doping specie near the growth interface. The kinetics of impurity incorporation are very much dependent upon the thermodynamic characteristics of the dopant species, its intermediate compounds, and the kinetics of surface incorporation.

Little is known of the incorporation kinetics of carbon in epitaxial GaAs, except that it is difficult to achieve. The details of carbon incorporation and the effect of reduced pressure on these kinetics depend on the doping species present at the top boundary layer interface. Little is known about that. This is also true of silicon in the present studies.

Zn doping from dimethylzinc has been studied and found to be controlled by the diffusion of the dopant through the stagnant boundary layer and its decomposed form. The sticking coefficient for zinc is low and increased gas velocities occurring in reduced pressure MOCVD are thought to be important in reducing its incorporation.

E. Ultimate Purity Obtainable by MOCVD

It would appear that the only inherent limitation to the purity of GaAs by MOCVD is the incorporation of carbon. The trends evident in this work are that lower growth temperatures will result in substantially lower concentrations of carbon both as donors and acceptors in the GaAs films. Based on the data of Fig. 7, we estimate that growth at temperatures as low as 500°C will result in GaAs films with total impurity concentrations below 10^{14} cm^{-3}. In order to achieve this low temperature growth, it will be necessary to increase the effective As partial pressure over the substrate at the substrate boundary layer. To do this, it may be necessary to consider alternative high purity sources of As such as elemental As, trimethylarsine, and $AsCl_3$. It is also possible that the conditions for growth which result in n-type film conductivity will require substantially lower growth rates owing to the lower effective As partial pressures.

F. Conclusions

The data presented in this paper show conclusively that with high purity starting materials and optimized growth procedures, high purity GaAs can be grown by MOCVD using trimethylgallium and arsine. Total impurity concentrations as low as $N_D + N_A = 5 \times 10^{14}$ cm^{-3} ($\mu_{77} = 125{,}000$ $cm^2/Vsec$) have been obtained by growth with high purity starting materials and at reduced pressures. Carbon, Silicon, and zinc are shown to be the dominant residual impurities in the material. Carbon is the only impurity inherent to the process and its incorporation can be reduced by growth at low temperatures. Total impurity concentrations below 10^{14} cm^{-3} are thought to be possible.

ACKNOWLEDGMENTS

The authors acknowledge the continued encouragement of Howard Lessoff, NRL, in providing support for this work. We also acknowledge the substantial technical assistance provided by J. J. Yang, H. H. Weider (NOSC), S. G. Bishop (NRL), and P. Klein (NRL) who provided important data inputs to this program.

REFERENCES

1. H. M. Manasevit and W. I. Simpson, J. Electrochem. Soc. 116 (1969) 1725.
2. H. M. Manasevit, Appl. Phys. Lett. 12 (1968) 156.
3. S. Ito, T. Shinohara, and Y. Seki, J. Electrochem. Soc. 120 (1973) 1419.
4. Y. Seki, K. Tanno, K. Iida, and E. Ichiki, J. Electrochem. Soc. 122 (1975) 1108.
5. R. D. Dupuis, P. D. Dapkus, R. D. Yingling, and L. A. Moudy, Appl. Phys. Lett. 31(1977) 201.
6. R. D. Dupuis and P. D. Dapkus, Appl. Phys. Lett. 31 (1977) 466.
7. R. D. Dupuis and P. D. Dapkus, Appl. Phys. Lett. 32 (1978) 437.
8. E. J. Thrush and J. E. A. Whiteaway, Proc. GaAs and Related Compounds Symposium 1980, p. 337.
9. R. D. Dupuis, P. D. Dapkus, N. Holonyak, Jr., E. A. Rezek, and R. Chin, Appl. Phys. Lett. 33 (1978) 596.
10. M. Allenson and S. J. Bass, Appl. Phys. Lett. 28 (1976) 113.
11. H. Morkoc, J. Andrews, and V. Aebi, Electron. Lett. 15 (1979) 106.
12. S. J. Bass, J. Cryst. Growth 31 (1975) 172.
13. G. B. Stringfellow and H. T. Hall, J. Cryst. Growth 43 (1978) 47.
14. G. B. Stringfellow and H. T. Hall, J. Electron Mat. 8 (1979) 201.
15. J. P. Duchemin, M. Bonnet, F. Koelsch, and D. Huyghe, J. Cryst. Growth 43 (1978) 181.
16. J. P. Duchemin, M. Bonnet, and F. Koelsch, J. Electrochem. Soc. 125 (1978) 637.

17. J. P. Duchemin, M. Bonnet, and G. Beuchet, J. Vac. Sci. Technol. 16 (1979) 1126.

18. G. E. Stillman, D. M. Larsen, C. M. Wolfe, and R. C. Brandt, Solid State Commun. 9 (1971) 2245.

19. R. A. Stradling, L. Eaves, R. A. Hoult, N. Miura, P. E. Simmonds, and C. C. Bradley, 1972 Proc. GaAs and Related Compounds, p. 65.

20. G. E. Stillman, D. M. Larsen, and C. M. Wolfe, Phys. Rev. Lett. 15 (1971) 989.

21. C. M. Wolfe, G. E. Stillman, and D. M. Korn, 1976 Proc. GaAs and Related Compounds, p. 120.

22. M. Ozeki, K. Kitahara, K. Nakai, A. Shibatomi, K. Dazai, S. Okawa, O. Ryuzan, Jpn. J. Appl. Phys. 16 (1977) 1617.

23. D. J. Ashen, P. J. Dean, D. T. J. Hurle, J. B. Mullin, and A. M. White, J. Phys. Chem. Solids 36 (1975) 1041.

24. C. M. Wolfe, G. E. Stillman, and J. O. Dimmock, J. Appl. Phys. 41 (1970) 504.

25. G. E. Stillman and C. M. Wolfe, Thin Solid Films 31 (1976) 69.

26. K. L. Hess, P. D. Dapkus, and H. M. Manasevit, unpublished.

27. H. M. Manasevit and A. C. Thorsen, J. Electrochem. Soc. 119 (1972) 99.

TABLE I. COMPARISON OF OPTIMIZED GROWTH PARAMETERS

OPTIMIZED GROWTH PARAMETER	ATMOSPHERIC PRESSURE	REDUCED PRESSURE
Reactor Pressure	760 torr	70 torr
Total Gas Flow	4.0 LPM	1.0 LPM
10% AsH_3/H_2 Flow	500 CCPM	500 CCPM
$H_2/(CH_3)_3Ga$ Bubbler Flow	15 CCPM	10 CCPM
$(CH_3)_3Ga$ Source Temperature	0°C	- 12°C
Growth Temperature	600 to 625°C	575 to 600°C
Growth Rate	~0.166 μm/min	0.055 μm/min

TABLE II

ENERGY OF 1S-2P ($m = -1$) TRANSITION (65 kG) FOR VARIOUS DONORS IN GaAs

Pb	35.0 cm^{-1}
X_1 (1)	35.3 cm^{-1}
Se	35.42 cm^{-1}
Sn	35.50 cm^{-1}
Si	35.90 cm^{-1}
S	36.37 cm^{-1}
C (2)	36.82 cm^{-1}
Ge (2)	36.7 cm^{-1}

(1) X_1 is a donor level observed in a variety of GaAs materials and is believed to be associated with Ga vacancy complex.

(2) There is some ambiguity in the identification of C and Ge donors. Recent work[i] identified the X_3 peak of Stillman, et al [ii] as due to Ge. The present work corroborates Stillman's early identification of X_3 as being C.

i M. Ozeki, et al, Jpn J. Appl. Phys., 16, 1617 (1977).

ii C. M. Wolfe, et al, *Proceedings of the GaAs and Related Compounds Conference, St. Louis, 1976,* Inst. of Phys., London and Bristol, p. 120.

TABLE III. EFFECT OF SOURCE PURITY ON 77°K MOBILITY

TMGa SOURCE	AsH_3 SOURCE	77°K MOBILITY (cm^2/Vsec)
TA-1	PR-1, PR-4	75,000 to 87,000
AV-1	PR-1	40,000 to 50,000
L-1	PR-4	20,000 to 30,000
TA-1	SG-1	38,000 to 45,000
TA-1	PR-2	~ 40,000
TA-1	PR-3	60,000 to 70,000
TA-1*	PR-4	~ 85,000
TA-1*	PR-1	~ 105,000

Growth Temperature - 600°C

Growth Rate -- 0.2 μm/min

* Redistilled

TABLE IV. ELECTRICALLY ACTIVE IMPURITIES

OBSERVED IN HIGH PURITY GaAs GROWN BY MOCVD

Donors Observed:	X_1, Si, C
Acceptors Observed:	C, Si, Zn

TABLE V. EFFECT OF AsH_3/TMGa RATIO ON ELECTRICAL PROPERTIES OF MOCVD GROWN GaAs

AsH_3/TMGa	$N_D-N_A(cm^{-3})$	$\mu(77°K)(cm^2/Vsec)$
39(1)	High Resistivity/p-type	
103(2)	2.8×10^{14}	101,353
180(3)	4.0×10^{14}	90,172
39(1)	High Resistivity/p-type	
103(2)	3.9×10^{14}	65,000
39(1)	9.5×10^{12}	10,618
103(2)	3.4×10^{14}	89,438

Growth Temperature: 600°C

10% AsH_3 Flow Rate: 500 cc/min

(1) H_2 flow rate through TMGa at 0°C -- 15 cc/min

(2) H_2 flow rate through TMGa at - 12°C -- 10 cc/min

(3) H_2 flow rate through TMGa at - 20°C -- 10 cc/min

TABLE VI. COMPARISON OF ELECTRICAL PROPERTIES OF UNDOPED MOCVD GROWN GaAs: ATMOSPHERIC PRESSURE VS REDUCED PRESSURE

Run #	REACTOR PRESSURE (torr)	SOURCES	$N_D-N_A(cm^{-3})$	$\mu(77°K)$ $(cm^2/Vsec)$
125	760	TA-1; PR-3	1.1×10^{14}	80,345
127	70		2.8×10^{14}	101,353
135	760	TA-1; PR-4	2.4×10^{14}	87,471
138	70		3.9×10^{14}	89,437
161	760	TA-1*; PR-4	5.5×10^{13}	68,439
165	70		3.9×10^{14}	105,582
S-1	760	TA-1*; PR-5	3.5×10^{14}	69,359
S-2	70		2.6×10^{14}	88,436
S-3	760	TA-1*; PR-7	6.5×10^{12}	103,774
S-4	70		5.4×10^{13}	125,200

FIGURE CAPTIONS

Fig. 1. Schematic diagram of MOCVD reactor

Fig. 2. (a) Schematic representation of photothermal ionization process operative in far infrared donor spectroscopy

(b) Photoconductivity spectra without magnetic field showing excited state transitions

(c) Photoconductivity spectra with magnetic field showing splitting of transitions

Fig. 3. Dependence of net carrier concentration upon As/Ga in MOCVD GaAs grown at atmospheric pressure

Fig. 4. Dependence of measured 77°K mobility upon film thickness

Fig. 5. Dependence of 77°K mobility upon growth temperature in > 20 μm thick films

Fig. 6. Dependence of residual donor (N_D), acceptor (N_A), and total impurity ($N_D + N_A$) concentrations upon growth temperature

Fig. 7. Far infrared photoconductivity donor spectra of MOCVD GaAs samples grown at atmospheric pressure and at various growth temperatures

Fig. 8. Comparative morphology of thick (> 30 μm) GaAs grown at atmospheric and reduced pressure

Fig. 9. Far infrared photoconductivity donor spectra of two GaAs samples grown under optimized conditions at reduced pressure

LOW PRESSURE MOCVD GROWTH REACTOR

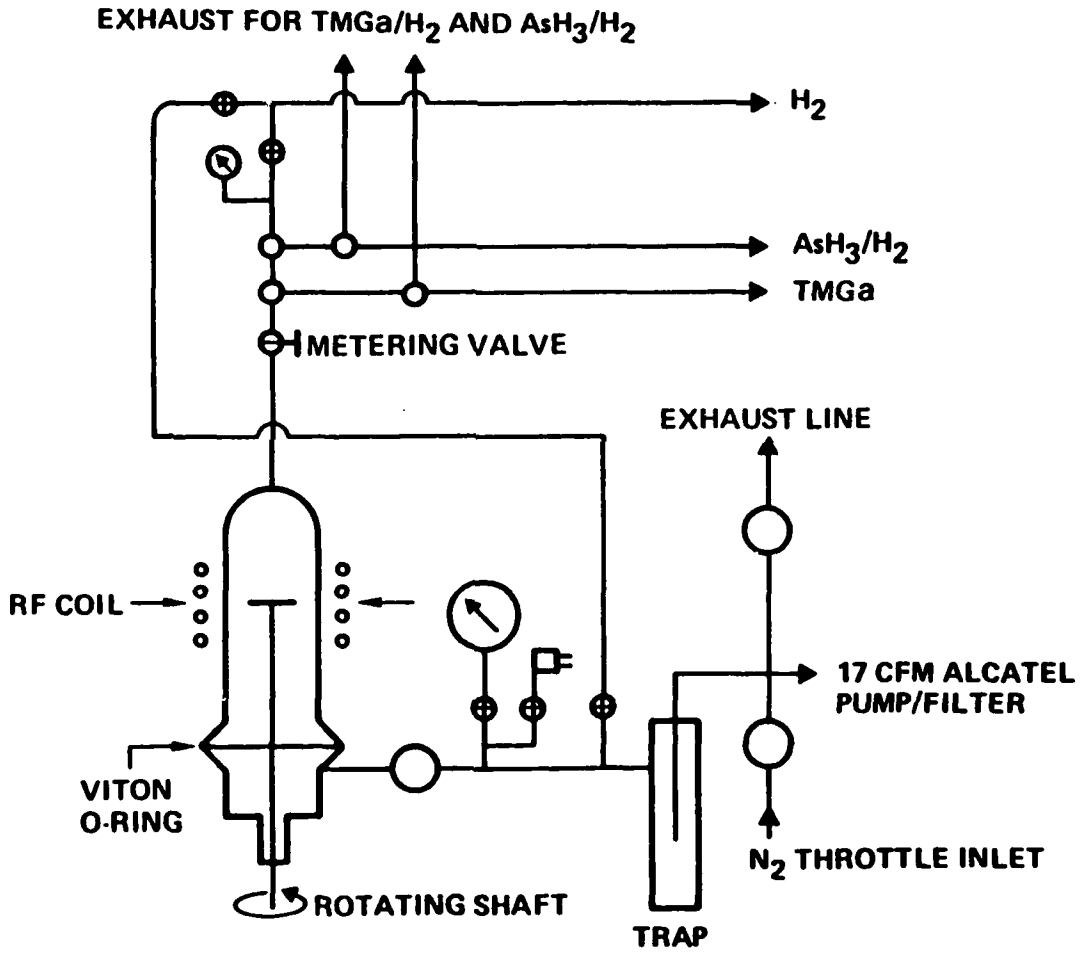

Figure 1

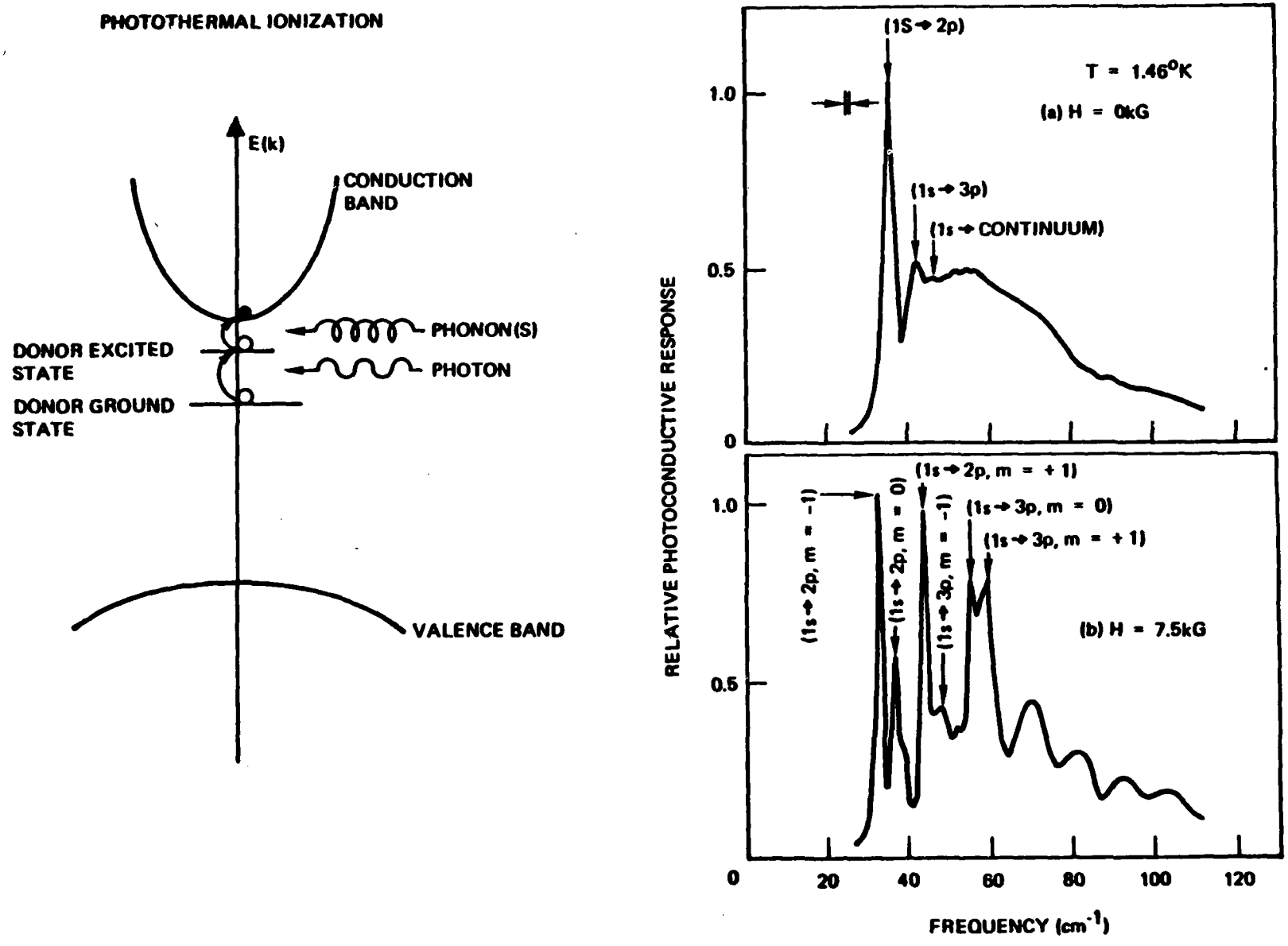
PHOTOTHERMAL IONIZATION
E(k)
CONDUCTION BAND
PHONON(S)
PHOTON
DONOR EXCITED STATE
DONOR GROUND STATE
VALENCE BAND
(1S→2p)
T = 1.46°K
(a) H = 0kG
(1s→3p)
(1s→CONTINUUM)
1.0
0.5
0
RELATIVE PHOTOCONDUCTIVE RESPONSE
(1s→2p, m = -1)
(1s→2p, m = 0)
(1s→2p, m = +1)
(1s→3p, m = -1)
(1s→3p, m = 0)
(1s→3p, m = +1)
(b) H = 7.5kG
20
40
60
80
100
120
FREQUENCY (cm⁻¹)

Figure 2

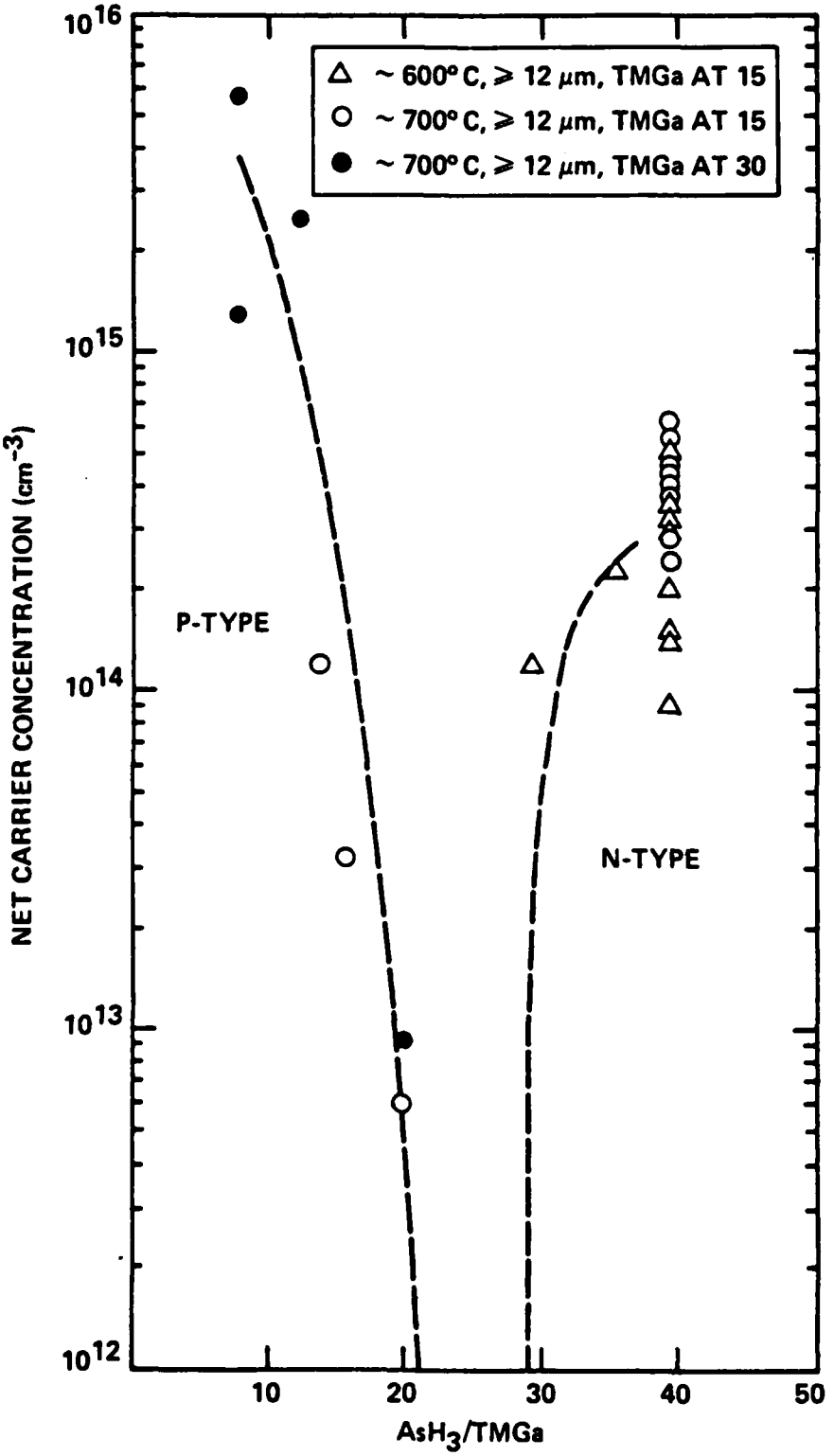
△ ~ 600° C, ≥ 12 μm, TMGa AT 15
○ ~ 700° C, ≥ 12 μm, TMGa AT 15
● ~ 700° C, ≥ 12 μm, TMGa AT 30
P-TYPE
N-TYPE
NET CARRIER CONCENTRATION (cm-3)
10^16
10^15
10^14
10^13
10^12
10
20
30
40
50
AsH3/TMGa

Figure 3

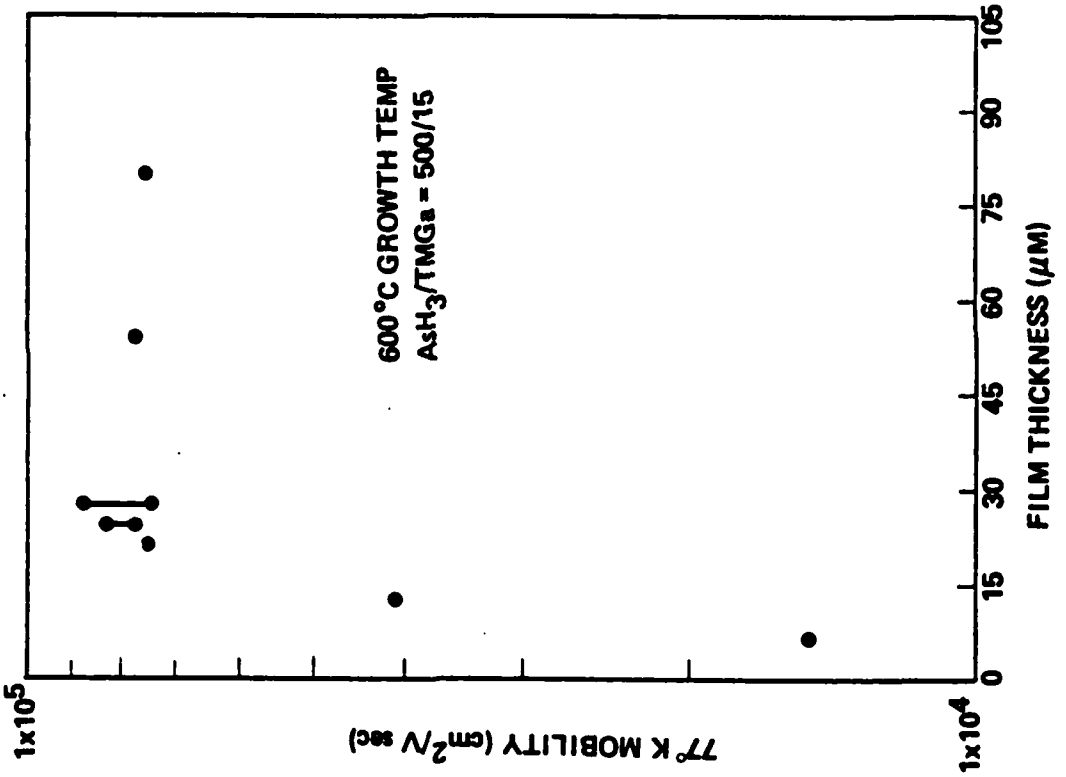
600°C GROWTH TEMP
AsH3/TMGa = 500/15
77° K MOBILITY (cm2/V sec)
1x10^5
1x10^4
0
15
30
45
60
75
90
105
FILM THICKNESS (μM)

Figure 4

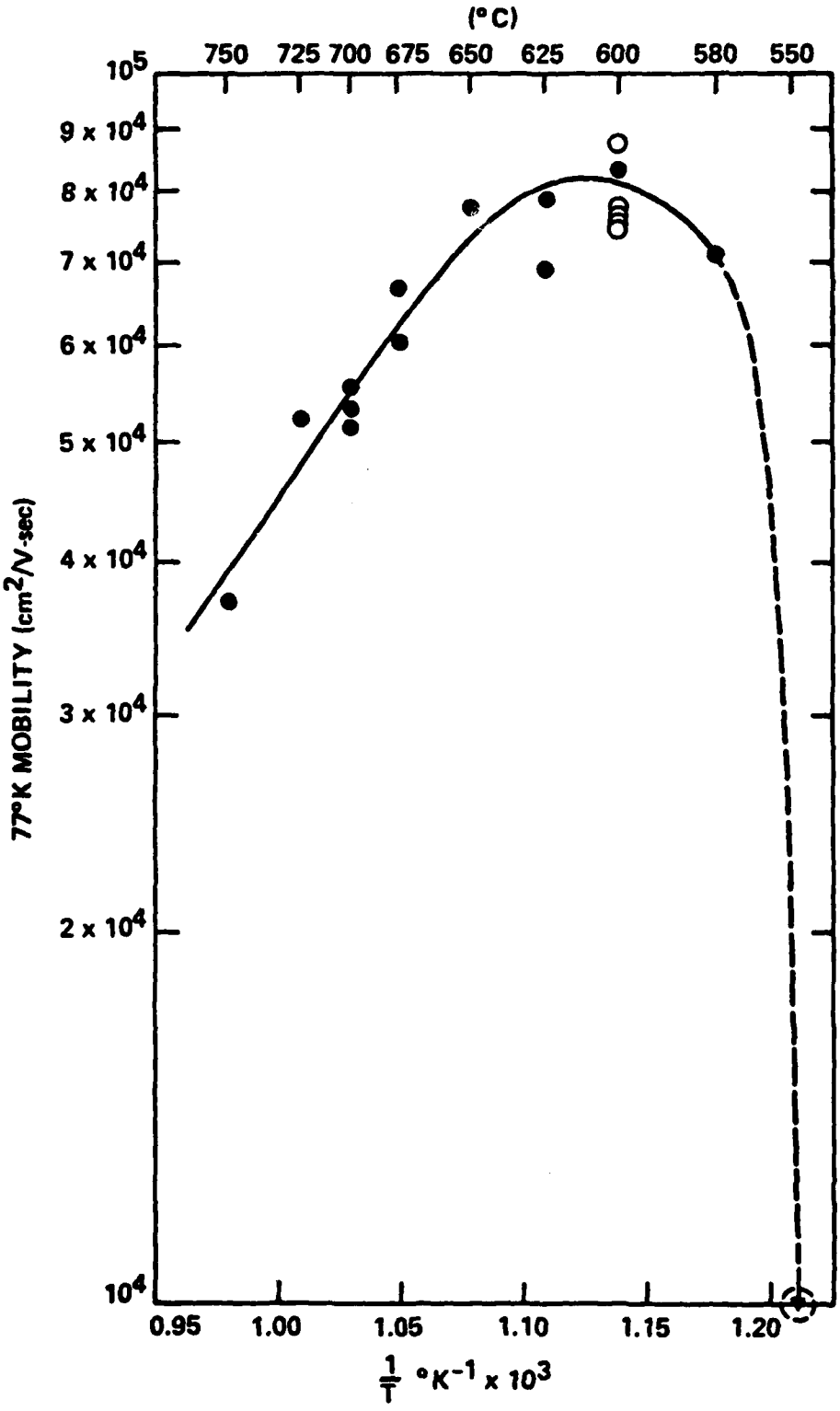
(°C)
750
725
700
675
650
625
600
580
550
10^5
9×10^4
8×10^4
7×10^4
6×10^4
5×10^4
4×10^4
3×10^4
2×10^4
10^4
77°K MOBILITY (cm^2/V-sec)
0.95
1.00
1.05
1.10
1.15
1.20
$\frac{1}{T}$ °K^{-1} x 10^3

Figure 5

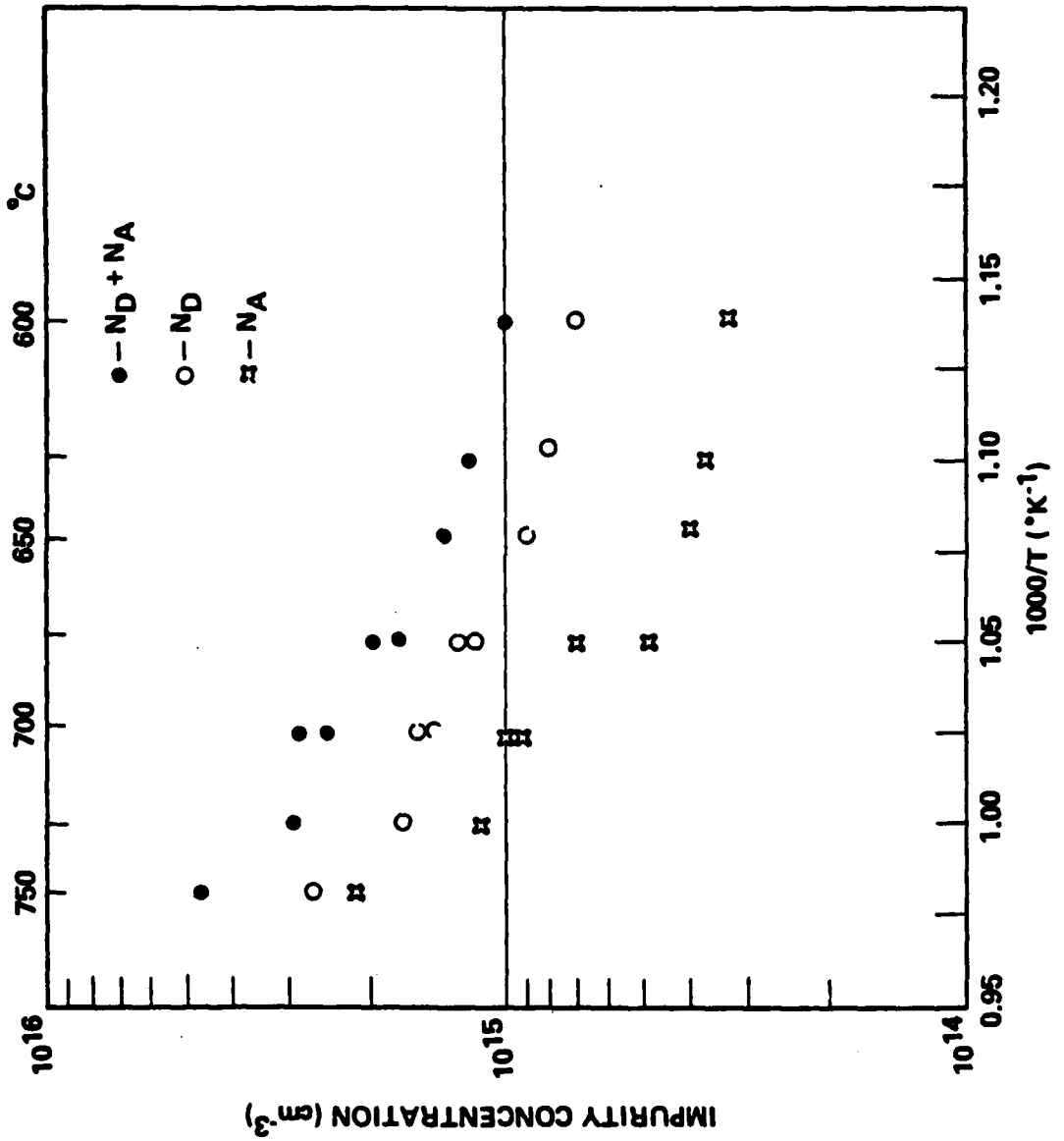
IMPURITY CONCENTRATION (cm⁻³)
10¹⁶
10¹⁵
10¹⁴
750
700
650
600
°C
0.95
1.00
1.05
1.10
1.15
1.20
1000/T (°K⁻¹)
● — N_D + N_A
○ — N_D
¤ — N_A

Figure 6

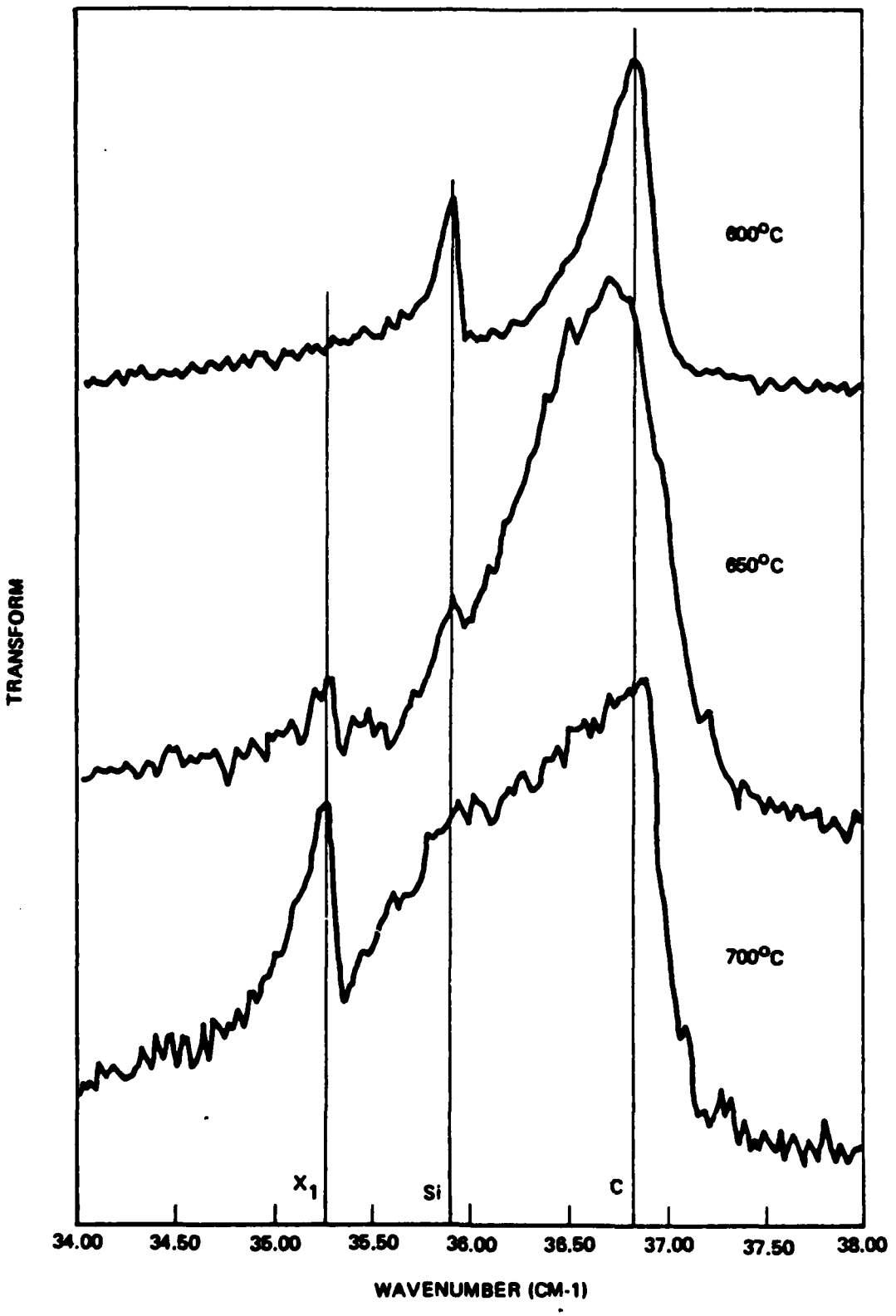
600°C
650°C
700°C
TRANSFORM
X1
Si
C
34.00
34.50
35.00
35.50
36.00
36.50
37.00
37.50
38.00
WAVENUMBER (CM-1)

Figure 7

ATMOSPHERIC PRESSURE MOCVD
FILM THICKNESS: 30 μM
GROWTH RATE: 0.25 μM/MIN

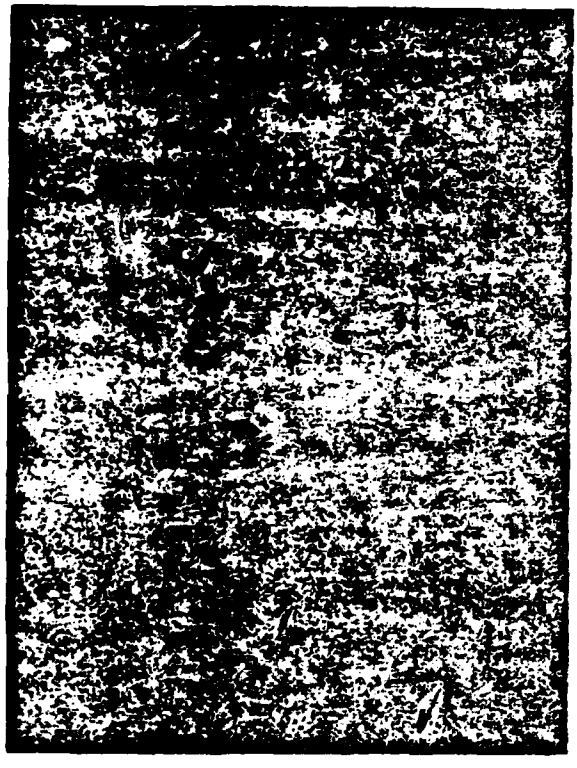

LOW PRESSURE MOCVD
FILM THICKNESS: 30.5 μM
GROWTH RATE: 0.07 μM/MIN

Figure 8